PUX10 is a CDC48A Adaptor Protein that Regulates the Extraction of Ubiquitinated Oleosins from Seed Lipid Droplets in Arabidopsis

Carine Deruyffelaere, Zita Purkrtova, Isabelle Bouchez, Boris Collet, Jean-Luc Cacas, Thierry T. Chardot, Jean-Luc Gallois, Sabine d'Andrea

RESEARCH ARTICLE

PUX10 is a CDC48A Adaptor Protein that Regulates the Extraction of Ubiquitinated Oleosins from Seed Lipid Droplets in Arabidopsis

Carine Deruyffelaere[a], Zita Purkrtova[a‡], Isabelle Bouchez[a], Boris Collet[a], Jean-Luc Cacas[a], Thierry Chardot[a], Jean-Luc Gallois[b], and Sabine D'Andrea[a]

[a]Institut Jean-Pierre Bourgin, INRA, AgroParisTech, CNRS, Université Paris-Saclay, 78000 Versailles, France

[b]GAFL, INRA, 84140 Montfavet, France

[‡]present adress: Department of Biochemistry and Microbiology, University of Chemistry and Technology, Prague, Czech Republic

Corresponding author: sabine.dandrea@inra.fr

Short title: Lipid droplet-associated degradation

One-sentence summary: PUX10 is a CDC48A adaptor associated with lipid droplets in germinating seeds and required for the extraction of ubiquitinated oleosins from lipid droplets, a prerequisite to oleosin degradation.

Material distribution footnote. The author responsible for distribution of materials integral to the findings presented in this article in accordance with the policy described in the Instructions for Authors (www.plantcell.org) is: Sabine D'Andrea (sabine.dandrea@inra.fr).

Abstract

Post-germinative mobilization of neutral lipids stored in seed lipid droplets (LDs) is preceded by the degradation of oleosins, the major structural LD proteins that stabilize LDs in dry seeds. We previously showed that *Arabidopsis thaliana* oleosins are marked for degradation by ubiquitination, and extracted from LDs before proteolysis. However, the mechanisms underlying the dislocation of these LD-anchored proteins from the LD monolayer are yet unknown. Here, we report that PUX10, a member of the plant UBX-domain containing (PUX) protein family, is an integral LD protein that associates with a subpopulation of LDs during seed germination. In *pux10* mutant seedlings, PUX10 deficiency impaired the degradation of ubiquitinated oleosins, and prevented the extraction of ubiquitinated oleosins from LDs. We also showed that PUX10 interacts with ubiquitin and CDC48A, the AAA ATPase Cell Division Cycle 48, through its UBA and UBX domains, respectively. Collectively, these results strongly suggest that PUX10 is an adaptor recruiting CDC48A to ubiquitinated oleosins, thus facilitating the dislocation of oleosins from LDs by the segregase activity of CDC48A. We propose that PUX10 and CDC48A are core components of a LD-associated degradation machinery, which we named the LD-associated degradation (LDAD) system. Importantly, PUX10 is also the first determinant of a LD subpopulation described in plants, suggesting functional differentiation of LDs in Arabidopsis seedlings.

Introduction

Essentially all cell types are able to synthesize and store neutral lipids. Storage lipids are packaged into specialized organelles called lipid droplets (LDs; also referred to as oil bodies, lipid bodies or oleosomes). Originally recognized for their importance in energy storage, LDs also play important roles in many cellular processes, including lipid transport and membrane synthesis, protein storage and degradation, lipid signaling, and stress response (Chapman and Trelease, 1991; Chapman et al., 2012; Murphy, 2012; Arrese et al., 2014; Welte and Gould, 2017; Huang, 2018).

The structure of LDs is unique among organelles and conserved across kingdoms, with a core of neutral lipids (mainly triacylglycerols and sterol esters) encircled by a phospholipid monolayer that contains specific proteins. Among the array of proteins identified in LDs isolated from different cell types and organisms, a specific set of structural proteins predominates. They belong to the oleosin (OLE) family in plant seeds, to the perilipin (PLIN) family in mammals, and to the major lipid droplet protein (MLDP) family in microalgae (D'Andrea, 2015; Goold et al., 2015; Bersuker and Olzmann, 2017).

In plants, besides the seed- and pollen-specific oleosins (Huang and Huang, 2015), a class of structural LD-associated proteins called lipid-droplet associated proteins (LDAPs; also abbreviated as SRPs) has recently been identified in non-seed tissues such as leaves and oleaginous fruit tissues (Gidda et al., 2013; Horn et al., 2013; Kim et al., 2016). Despite the absence of primary sequence similarity, these different families of structural LD proteins share a common role in controlling lipid mobilization. Overexpression and deficiency experiments support this notion. Indeed, overexpression or ectopic expression of oleosins, perilipins or LDAPs consistently induces the accumulation of neutral lipids (Brasaemle et al., 2000; Jamme et al., 2013; Gidda et al., 2016). This accumulation could result from either reduced lipolysis or increased LD formation, but the latter hypothesis is unlikely in plants because oleosin or LDAP deficiency induces limited to no decrease in triacylglycerol accumulation (Miquel et al., 2014; Gidda et al., 2016). Oleosins, perilipins and LDAPs may prevent lipolysis by covering the entire LD surface and shielding triacylglycerols from lipases. They can also

regulate lipolysis by interacting with cytoplasmic lipases and regulatory proteins, a well-documented role for perilipins but probably not fulfilled by oleosins (D'Andrea, 2015; Sztalryd and Brasaemle, 2017).

How these major LD proteins are removed from the LD surface to allow the turnover of storage lipids remains largely an unanswered question. Part of the answer depends on how these proteins interact with the LD surface. According to Kory et al. (2016), LD-associated proteins can be classified into two groups based on how they target LDs. Class II LD proteins access the LD surface from the cytosol and bind through amphipathic helices or domains. PLINs are recognized as class II LD proteins (Kory et al., 2016; Rowe et al., 2016). LDAPs may belong to this class as they localize predominantly to the cytosol when overexpressed in cells lacking abundant LDs, but the mechanism for their LD association is currently unknown (Gidda et al., 2016). By contrast, class I LD proteins are co-translationally inserted into the endoplasmic reticulum (ER) and translocated from the ER to nascent LDs (which originated by the accumulation of neutral lipids between the two leaflets of the ER membrane bilayer) or to expanding LDs through ER-LD membrane bridges (Wilfling et al., 2013). Class I proteins are embedded into the LD monolayer by hydrophobic sequences that frequently adopt a hairpin topology. Contrary to class II proteins, they cannot translocate from LDs to the cytosol and must be removed from LDs by a specific, yet unknown mechanism.

Oleosins are the first identified and best structurally described class I LD proteins. Co-translationally inserted in ER-budding LDs, they exclusively localize to LDs through a hydrophobic hairpin domain that deeply penetrates into the LD core (Beaudoin and Napier, 2002; Huang and Huang, 2017). This hairpin, consisting of a conserved 72-residue hydrophobic region with a central proline knot, is indeed too long to be stable in the phospholipid bilayer of a membrane. Seed oleosins have short hydrophilic N- and C-terminal peptides flanking the central hydrophobic hairpin and exposed to the LD surface (Jolivet et al., 2017). This amphipathic tri-block structure is probably responsible for the ability of oleosins to reduce interfacial tension at the oil/water interface *in vitro* (Roux et al., 2004) and to stabilize LDs *in vivo*. In mature seeds, oleosin deficiency is

indeed associated with giant LDs instead of normal submicrometer-sized LDs, showing that oleosins control LD size and stability by preventing LD coalescence during desiccation (Siloto et al., 2006; Schmidt and Herman, 2008; Miquel et al., 2014).

In *Arabidopsis thaliana* seeds, the degradation of the oleosin coat surrounding LDs begins during seed germination (Deruyffelaere et al., 2015). Oleosin proteolysis thus starts before lipid mobilization, which occurs post-germinatively to sustain seedling growth before the onset of photosynthesis. This observation suggests that proteolysis of oleosins is a prerequisite for lipolysis and brings up the question of how these class I LD proteins are degraded. Previous studies have shown that oleosins are marked for degradation by ubiquitination (Hsiao and Tzen, 2011; Deruyffelaere et al., 2015). The ubiquitination profile of oleosins in germinating seeds is surprisingly complex. Three distinct and exclusive motifs can be attached to the most abundant Arabidopsis oleosins OLE1 and OLE2: monoubiquitin, K48-linked diubiquitin chain, and K63-linked diubiquitin chain (Deruyffelaere et al., 2015). These different ubiquitinations may channel modified oleosins towards specific degradation pathways according to ubiquitination type. One of these pathways was identified as the ubiquitin-proteasome pathway, which specifically degrades oleosins marked by the addition of a K48-linked diubiquitin. Once ubiquitinated, these oleosins are extracted from the LD coat before proteasomal degradation (Deruyffelaere et al., 2015). However, the molecular mechanism underlying oleosin extraction still remains unknown.

Proteomic analyses of seed LDs revealed two candidate proteins that could be involved in this mechanism. One candidate is a putative ubiquitin-binding protein belonging to the plant UBX-domain containing (PUX) protein family, named PUX10. The other candidate is a putative PUX10 interactant called cell division cycle 48 homolog A (CDC48A). CDC48A is a chaperone-like ATPase known for its role in the ER-associated degradation (ERAD) of misfolded proteins (Liu and Li, 2014). We showed that *PUX10* mutations impair the degradation of all three types of ubiquitinated oleosins, and prevent the dislocation of ubiquitinated oleosins from LDs, which precedes LD degradation. Our results also revealed that PUX10 is an integral LD protein that acts as an adaptor recruiting CDC48A to ubiquitinated oleosins, thus facilitating the dislocation

of oleosins from LDs by the segregase activity of CDC48A. We propose that PUX10 and CDC48A are core components of a LD-associated ERAD-like degradation machinery, which we named LD-associated degradation (LDAD).

Results

PUX10 and CDC48A, two candidates for oleosin extraction from LDs

To gain insight into the proteins involved in LD dynamics in seeds, we previously performed a proteomics analysis of LDs isolated from *Arabidopsis thaliana* seeds at various post-germinative stages (Deruyffelaere et al., 2015). A search for candidates involved in the degradation of ubiquitinated oleosins only resulted in the identification of a putative ubiquitin-binding protein called PUX10 and the CDC48A ATPase (Supplemental Data Set 1 and Supplemental Figure 1). The latter protein belongs to a family of highly conserved ATPases named AAA-ATPases (ATPases associated with various cellular activities) involved in many processes ensuring cellular homeostasis, including protein degradation by the ubiquitin-proteasome system (UPS) and by autophagy (Barthelme and Sauer, 2016). Members of the CDC48 family (called Cdc48 in yeast and p97 or VCP in metazoans) are considered to mediate these functions through their ubiquitin-selective segregase activity that separates ubiquitinated proteins from binding partners or cellular structures (Jentsch and Rumpf, 2007). CDC48 proteins indirectly associate with ubiquitinated substrates through cofactors. These substrate-recruiting cofactors bind CDC48s via specific interaction domains like the ubiquitin regulatory X (UBX) domain.

PUX10 contains a putative UBX domain at its C terminus (Figure 1A and Supplemental Figure 2), indicating that it may act as a CDC48A cofactor. The Arabidopsis genome encodes 16 UBX-containing proteins (called PUX1-16) and four of them (PUX1, PUX4, PUX5 and PUX7) have so far been shown to interact with CDC48A (Rancour et al., 2004; Park et al., 2007; Gallois et al., 2013). PUX10 also contains a UBA-like domain, which is known to bind ubiquitin (Hurley et al., 2006). As such, it appears that PUX10 may have a role in the degradation of oleosins as an adaptor bridging ubiquitinated oleosins to CDC48A. The hypothesis of a role of PUX10 in LD degradation is

strengthened by the observation that PUX10 is the closest putative Arabidopsis ortholog of mammalian FAF2/UBXD8 and yeast Ubx2p, two LD-associated proteins known to control LD dynamics (Suzuki et al., 2012; Wang and Lee, 2012; Olzmann et al., 2013). Indeed, PUX10 clusters in the same phylogenetic group as FAF2/UBXD8 and Ubx2p, unlike the other Arabidopsis PUXs (Supplemental Figure 3; Supplemental Dataset 2). PUX10 is also the only Arabidopsis PUX containing a putative membrane-anchoring domain, as predicted by CCTOP algorithms (http://cctop.enzim.ttk.mta.hu). The two membrane-anchoring domains detected in PUX10 (amino acid residues 102-117 and 120-141, highlighted in yellow in Supplemental Figure 2) may form a hydrophobic hairpin, which is a characteristic structure of class I LD proteins (Thiam et al., 2013; Kory et al., 2016). Such a hairpin domain, sometimes referred to as the HP domain, is present in UBXD8 and Ubx2p and required for membrane and LD targeting (Lee et al., 2010; Wang and Lee, 2012). Moreover, PUX10 displays a domain architecture similar to that of UBXD8 and Ubx2p, with the hydrophobic region located between the N-terminal UBA domain and the central UAS domain (Figure 1A and Supplemental Figure 2).

Taken together, these data highlight PUX10 and CDC48A as good candidates for controlling oleosin degradation during LD mobilization. To explore their role in LD dynamics, we have undertaken functional analyses using T-DNA mutants. Because CDC48A-deficient mutants were reported to be lethal (Park et al., 2008), we focused our study on PUX10 mutants.

Isolation and characterization of *pux10* mutants

Two T-DNA insertion mutants were isolated from the SAIL and FLAG collections and called *pux10-1* (SAIL_1187) and *pux10-2* (FLAG_211E02). The T-DNA inserts of *pux10-1* and *pux10-2* mutants mapped to the first and third exons, respectively (Figure 1A (left)). We analyzed *PUX10* expression by RT-PCR in mutant backgrounds. As expected, RT-PCR amplification using primers on either side of the T-DNA insertion site occurred in Columbia (Col-0) and Wassilewskija (Ws) accessions but not in *pux10-1* or *pux10-2* mutants (Figure 1A (right); F4-R3 and F5-R2 PCRs for *pux10-1*; F4-R3 and F3-R3 PCRs for *pux10-2*). However, DNA fragments were amplified from *PUX10* transcripts in mutant backgrounds when primers located upstream (F5-R2 for *pux10-2*)

or downstream (F3-R3 for *pux10-1*, and F9-R3 for *pux10-1* and *pux10-2*) of the T-DNA insertion site were used (Figure 1A). This result indicates that *pux10-1* and *pux10-2* may not be knockout mutants, as modified *PUX10* transcripts are synthesized and may possibly be translated into aberrant proteins in these insertional lines.

The effect of *PUX10* mutation on lipid accumulation during seed maturation was assessed by measuring the average weight and the fatty acid (FA) content of *pux10-1* and *pux10-2* mature seeds. No significant difference between mutant genotypes and their respective wild types was observed for these parameters (Supplemental Figure 4A-B). By contrast, FA composition was altered in both *pux10* mutants (Supplemental Figure 4C). The relative abundance of linoleic acid (C18:2) slightly but significantly decreased with a concurrent increase in linolenic acid (C18:3) levels. Consequently, the ratio of C18:3 to C18:2 was consistently increased in *pux10* mutants (Supplemental Figure 4D), suggesting a role for PUX10 in polyunsaturated FA metabolism during seed maturation. We also analyzed phenotypic effects of the mutations affecting *PUX10* on seed germination and plant growth. Germination rates were similar between *pux10* mutants and their wild-type counterparts (Supplemental Figure 4E). The absence of a developmental phenotype thus allowed rigorous comparison between mutant and wild-type plants at different stages of seed germination and seedling growth.

PUX10 mutation impairs oleosin degradation in young seedlings

During germination and early seedling growth, oleosins are targeted for degradation by ubiquitination (Deruyffelaere et al., 2015). To explore the potential role of PUX10 in the degradation of ubiquitinated oleosins, we evaluated the content of ubiquitinated oleosins in *pux10* and wild-type seedlings at various post-germinative stages. We analyzed by immunoblotting the three types of oleosin ubiquitinations previously described in germinating seeds (Deruyffelaere et al., 2015). Oleosins marked for proteasomal degradation by the addition of a K48-linked diubiquitin (hereafter referred to as OLEs-K48Ub_2) over-accumulated in *pux10-1* and *pux10-2* germinating seeds compared to their respective wild types (Apu2 immunoblots; Figure 1B). This accumulation was not only more intense but also lasted longer, suggesting that PUX10 is required for OLEs-K48Ub_2 to enter the UPS degradative pathway. The mutations in *PUX10* also reduced

the degradation of the two other types of ubiquitin-oleosin conjugates, i.e. monoubiquitinated oleosins (OLEs-Ub) and oleosins marked with a K63-linked diubiquitin (OLEs-K63Ub$_2$). Indeed, immunodetection of OLEs-Ub and OLEs-K63Ub$_2$ using FK2 and Apu3 antibodies, respectively, revealed a strong accumulation of these two types of ubiquitinated oleosins in 24-h- to 50-h-old seedlings, associated with *PUX10* mutation (Apu3 and FK2 immunoblots; Figure 1B). Overall, these results demonstrate that PUX10 is involved in the degradation of all types of ubiquitinated oleosins, without discriminating between the three ubiquitination motifs borne by oleosins. It is noteworthy that both insertional mutations in *PUX10* substantially reduced, but did not block, the degradation of ubiquitinated oleosins. This partial phenotype suggests that ubiquitinated oleosins could be proteolyzed by a yet unidentified PUX10-independent degradation pathway (this hypothesis is detailed in the discussion). An alternative explanation is that *pux10-1* and *pux10-2* are not null mutants but hypomorphic ones, as suggested by the RT-PCR analysis previously described (Figure 1A).

To confirm the role of PUX10 in the ubiquitin-dependent proteolysis of oleosins, we analyzed the degradation of native oleosins during post-germinative seedling growth. Between 32 h and 50 h of germination, the gradual hydrolysis of oleosins was slower in *pux10-1* and *pux10-2* mutants than in their corresponding wild-type seedlings, as shown by Coomassie-stained SDS-PAGE of seed proteins (Figure 1B; Coom. panels) and by specific immunodetection of the two major oleosins, OLE1 and OLE2 (Figure 1B; OLE1 and OLE2 immunoblots). Quantification of OLE1 in 41-h-old seedlings confirmed the significant reduction of OLE1 hydrolysis in the *pux10-1* mutant compared to Col0 (Figure 1C; left panel). We conclude that *PUX10* mutation impairs the degradation of ubiquitinated oleosins, which results in a significant reduction of oleosin hydrolysis in young seedlings.

PUX10 mutation alters LD size but not oil mobilization in young seedlings

To further characterize the effects of PUX10 on post-germinative LD degradation, we analyzed the oil content of mutant and wild-type seedlings by measuring eicosanoic acid (C20:1), a FA specific to storage oil. Eicosanoic acid content was not significantly

different between *pux10-1* and Col0 seedlings at 41 h of germination (Figure 1C; right panel), contrary to OLE1 content (Figure 1C; left panel). The degradation of the oleosin coat surrounding LDs and shielding oil from lipases is probably not impaired enough to prevent lipolysis in *pux10-1*. Although *PUX10* mutation did not significantly alter the amount of lipids packed in LDs, it had a major effect on LD size. To compare LD morphology between mutants and wild types, we stained neutral lipids of 32-h-old seedlings using LipidTOX Deep Red and then imaged LDs in epidermal cells of the lower hypocotyl by confocal laser-scanning microscopy (CLSM). Bright-field microscopy was also helpful to visualize LD rim. The left panel in Figure 1D displays representative images showing that LD size was smaller in mutants than in wild types. To quantify this difference, LD diameters were measured using ImageJ on several merged bright-field and confocal images. The boxplot representation of diameter distribution in Figure 1D (right panel) shows that LD size was significantly different between *pux10* mutants (0.69±0.27 and 0.70±0.23 µm for pux10-1 and pux10-2, respectively) and their corresponding wild types (1.85±0.61 and 1.62±0.53 µm for Col0 and Ws, respectively) as estimated by *t*-test ($p<0.0001$). This result suggests that *PUX10* mutation prevents the increase in LD size occurring during seed germination. LD morphology is indeed dramatically modified during germination (Miquel et al., 2014). Whereas LDs are very small in dry mature seeds (they cannot be individually distinguished by CLSM), they increase in size and reduce in number after seed imbibition and germination. Such a process most probably involves LD fusions that could be promoted by an increase in interfacial tension due to oleosin removal from the LD surface. We therefore hypothesize that the effect of *PUX10* mutation on LD size is indirect and results from the partial blockade of oleosin degradation.

Phenotypical restoration by PUX10-GFP and PUX10-myc

A transgenic complementation strategy was employed to confirm that the loss of function of *PUX10* is responsible for the mutant phenotype. The *pux10-1* mutant was transformed with constructs containing *ProPUX10:PUX10* (a 2907-bp genomic fragment encompassing 628 bp upstream of the coding sequence) and allowing the native promoter-driven expression of PUX10 C-terminally fused to GFP or myc. One stable

homozygous transgenic line was studied for each construct. Regardless of the tag, the restored expression of PUX10 was able to abolish the accumulation of ubiquitinated oleosins observed in 41-h-old *pux10-1* seedlings (Apu2, Apu3, and FK2 immunoblots in Figure 2A). Moreover, oleosin level in transgenic seedlings was similar to that of wild-type seedlings and lower than that of *pux10-1* seedlings (OLE1 and OLE2 immunoblots in Figure 2A), showing that PUX10 expression was able to restore normal oleosin degradation in the *pux10-1* mutant. Finally, we analyzed the capacity of PUX10-GFP to complement the LD size phenotype of *pux10-1* seedlings (Figure 2B). LDs of 32-h-old seedlings were significantly larger in the *ProPUX10:PUX10-GFP*/*pux10-1* transgenic line (1.38±0.56 µm in diameter) than in the *pux10-1* mutant (0.69±0.27 µm) as determined by *t*-test ($p<0.0001$). Expression of PUX10-GFP in the *pux10-1* mutant was therefore able to restore the increase in LD size occurring during seed germination in the wild-type background. The restoration was partial since LD size was smaller in transgenic (1.38±0.56 µm) than in wild-type (1.85±0.61 µm) seedlings, suggesting that PUX10 activity might be slightly decreased by the tag fused at its C-terminus, close to the UBA domain. Collectively, these results unambiguously demonstrate that the phenotype displayed by *pux10-1* seedlings is caused by the mutation affecting *PUX10*.

PUX10 associates with LDs during germination

Since the PUX10-GFP fusion protein complements the *pux10-1* loss-of-function, it is highly likely that the translational fusion is targeted similarly as the endogenous PUX10. Accordingly, we characterized the temporal and tissue-specific regulation of PUX10 and its subcellular localization by CLSM imaging of the fluorescent PUX10-GFP expressed in *ProPUX10:PUX10-GFP*/*pux10-1* transgenic lines. Three distinct homozygous transgenic lines of Arabidopsis were analyzed (lines #5, #7, and #12). As these three lines displayed similar patterns of localization (Supplemental Figure 5), a more detailed analysis was conducted on only one of them (line #12), which was the transgenic line characterized in the complementation experiment.

Our previous analysis of the LD proteome revealed an association of PUX10 with LDs in germinated seeds (Supplemental Figure 1). To confirm this subcellular localization, the fluorescent signal of PUX10-GFP relative to that of LipidTOX-stained LDs was imaged

in transgenic seeds by CLSM. At the beginning of germination, PUX10-GFP labelled punctate structures, less numerous in cotyledons than in the hypocotyl (Figure 3A; 4 h of germination). As these submicrometer-sized structures were scattered throughout LD clusters, they were assumed to be LDs that could not be individually distinguished by CLSM. This hypothesis was confirmed by imaging seeds at later stages of germination, when LDs get larger. In the hypocotyl and cotyledon epidermises of young seedlings at 24 h (Figure 3A) and 32 h of germination (Figure 4), the fluorescent PUX10-GFP uniformly labeled the entire circumference of LDs, as expected for a LD-associated protein. Notably, PUX10-free LDs (empty arrowheads) were present together with PUX10-coated LDs (white arrowheads) within a given cell (Figure 3A; 24 h of germination). We thus conclude that PUX10 exclusively localizes to LDs and only associates with a subset of LDs in the cotyledons and hypocotyl of germinating seeds. Moreover, PUX10 labelling was more intense at 24 h than at 4 h of germination, indicating an increase in PUX10 level during germination. This up-regulation was consistent with transcriptomic data retrieved from the eFP browser (Figure 3B) and was confirmed by immunoblot quantification of PUX10-GFP in transgenic *ProPUX10:PUX10-GFP*/*pux10-1* seeds/seedlings (Figure 3C). Overall, these results indicate that PUX10 is progressively expressed and unevenly targeted to cotyledon and hypocotyl LDs as germination progresses.

To characterize the tissue-specific regulation of PUX10, PUX10-GFP labeling was examined in different tissues of 32-h-old seedlings, revealing a brighter fluorescence in the radicle, collet (also called hypocotyl-radicle transition zone), and root hairs than in the cotyledons and hypocotyl (Figure 4; left panel). In the radicle and collet (including root hairs), PUX10 encircled the LipidTOX-stained lipid core, indicating that PUX10 was targeted to the surface of LDs in these tissues (Figure 4; right panels). PUX10 was therefore associated with LDs in newly germinated seedlings, whatever the tissue. However, we noticed major differences in PUX10 intracellular distribution between seedling tissues. Whereas PUX10 was associated with most, if not all, the LDs in the radicle, collet and root hairs, it was targeted to only a subset of LDs in the cotyledons and hypocotyl. Moreover, the intracellular positioning of LDs varied substantially between cell types. LDs localized to the cell periphery in cotyledon and hypocotyl

epidermises, as they did in dry mature seeds. By contrast, cells from the hypocotyl-radicle transition zone (including root hairs) and from the radicle exhibited one or a few central clustered pools of LDs (Figure 4; right panels).

PUX10 localization changes from LDs to chloroplasts during seed development

Publicly available expression data indicate that *PUX10* transcripts are not only present in dry and imbibed seeds but also in developing seeds, albeit to a lower extent (Figure 3B). This observation prompted us to decipher PUX10 expression and localization during seed development. Figure 3A shows that PUX10 was indeed expressed during embryogenesis, at 7 and 9 days after flowering (DAF), and during seed maturation, at 12 DAF. Surprisingly, PUX10 localization dramatically changed during the transition between seed embryogenesis and maturation. In the cotyledons and hypocotyl of embryos at the torpedo and upturned-U stages (7 and 9 DAF, respectively), PUX10 was targeted to the periphery of LDs. Three days later, in the mid-phase of oil accumulation (Baud et al., 2002), PUX10-GFP was no longer localized to LDs but labeled the chloroplast periphery, suggesting its association with the chloroplast membranes (Figure 3A; 12 DAF). We also observed a faint reticulated PUX10 fluorescence, distinct from the ring-shaped pattern typical of LD-associated proteins, suggesting an endoplasmic reticulum (ER) localization of PUX10 at 12 DAF. Along with the modification of PUX10 targeting, major changes occurred on LD structure during the embryogenesis-maturation transition. Whereas LDs were organized in central clusters during seed embryogenesis (7 and 9 DAF), they increased in size and were pushed towards the cell periphery at the maturation phase (12 DAF). These observations revealed that LDs are highly dynamic organelles during seed development and that PUX10 specifically associates with LDs during embryogenesis but no longer during seed maturation.

The hydrophobic HP domain of PUX10 is a membrane-anchoring sequence required for LD localization

To confirm the *in planta* association of PUX10 to LDs, mCherry fluorescent PUX10 was transiently expressed in *Nicotiana benthamiana* leaves together with GFP-tagged Arabidopsis OLE1 (GFP-OLE1), a LD marker. Consistent with its localization to LDs in

Arabidopsis early developing embryos and young seedlings, PUX10 was localized to OLE1-labeled LDs in *N. benthamiana* leaves (Figure 5A). Time-lapse imaging of GFP-PUX10 in *N. benthamiana* leaves revealed that PUX10-labeled LDs were dynamic organelles, permanently connected to and continuously moving along the ER (Supplemental Movie 1). Besides this association with LDs, PUX10 was localized to the chloroplast periphery (Figure 5A), as already observed in Arabidopsis developing seeds at the maturation phase (12 DAF; Figure 3A). Using transgenic *N. benthamiana* expressing an ER fluorescent marker, we observed that GFP-tagged PUX10 was also marginally localized to the ER (Figure 5B). Overall, these results show that GFP-PUX10 and mCherry-PUX10 fusions transiently expressed in *N. benthamiana* under the 35S promoter localize to the same subcellular compartments as the PUX10-GFP fusion expressed in Arabidopsis under the *PUX10* native promoter. These data reinforce the conclusion that PUX10 can be targeted to the membrane of LDs, chloroplasts, or ER.

PUX10 possesses two consecutive hydrophobic regions (I^{102}-V^{117} and I^{121}-F^{141}) that may form a membrane-anchoring hairpin-structured domain. To decipher the role of this hydrophobic domain, hereafter called HP domain because of its putative hairpin structure, we examined the effect of deleting this region on PUX10 localization in *N. benthamiana* cells. Whereas full-length PUX10 was targeted to LD, ER and chloroplast membranes (Figure 5B), a mutated version of PUX10 devoid of the HP domain (ΔI^{102}-F^{141}) was diffusely distributed in the cytoplasm, as expected for a cytosolic protein (Figure 5C). These results indicate that the HP domain is required for the association of PUX10 with monolayer and bilayer membranes.

The UBX domain of PUX10 promotes CDC48A association with LDs

The analysis of the LD proteome described above identified the AAA-ATPase CDC48A as a putative PUX10 interactant (Supplemental Data Set 1 and Supplemental Figure 1). To demonstrate this hypothesis, we first investigated whether CDC48A is associated with LDs in germinating seeds and young seedlings, especially as such a LD localization of CDC48A was not observed by Park and co-workers (Park et al., 2008). These authors analyzed the localization of CDC48A in complemented *Atcdc48A* mutant seedlings expressing YFP-AtCDC48A under the native *CDC48A* promoter

(*ProCDC48A:YFP-CDC48A/Atcdc48A* line). They only reported a nuclear and cytoplasmic localization of CDC48A and mentioned its recruitment to the division mid-zone during cytokinesis. To specifically assess the issue of CDC48A association with LDs, we reexamined CDC48A localization in seedlings from this *ProCDC48A:YFP-CDC48A/Atcdc48A* transgenic line, after fluorescent staining of LDs. Figure 6A shows that YFP-CDC48A fusion protein uniformly labeled the surface of some, but not all, LDs in cotyledon and hypocotyl epidermises of 32-h-old seedlings. To rule out a mislocalization artifact due to the presence of the GFP tag, we analyzed the association of the native CDC48A protein with purified LDs. Using specific antibodies, CDC48A was immunodetected in LDs isolated from dry mature and germinated seeds (Figure 7A), confirming the association of CDC48A to LDs. To characterize the biophysical interaction between CDC48A and LDs, purified LDs were washed in 8 M urea/carbonate buffer to release non-integral proteins. Under these conditions, CDC48A was released from LDs (Figure 7A), which is consistent with previous data showing that it is a peripheral membrane protein (Rancour et al., 2002). By contrast, PUX10 remained in the LD fraction after the washing step (Figure 7A), demonstrating that PUX10 is an integral LD membrane protein.

Both CDC48A and PUX10 are associated with a subset of LDs in Arabidopsis seedlings. This observation suggests that CDC48A and PUX10 may co-localize to some LDs during early seedling growth. To investigate this hypothesis, PUX10-GFP and mCherry-CDC48A protein fusions were transiently co-expressed in *N. benthamiana* leaves. As shown in Figure 6B (upper panel), fluorescent CDC48A co-localized with PUX10 to dots previously identified as LDs (in Figure 5A) and to chloroplast membranes. CDC48A also localized in the cytosol, albeit to a weaker extent. Disruption of the UBX domain of PUX10 abrogated the co-localization of CDC48A with PUX10 on LDs and chloroplast membranes (Figure 6B; middle panel), showing that the UBX domain is required for PUX10-mediated targeting of cytosolic CDC48A to membranes. To confirm that PUX10 mediates the membrane targeting of CDC48A, CDC48A was expressed without PUX10. In the absence of PUX10, CDC48A was indeed exclusively cytosolic and did not localize to OLE1-labeled LDs or chloroplast membranes (Figure 6B; lower panel). However, the role of PUX10 in mediating CDC48A targeting to LDs

could not be confirmed in Arabidopsis seeds. The association of CDC48A with LDs, measured by CDC48A immunodetection in purified seed LDs, was not impaired in *pux10* mutants (Figure 7B). To explain this apparent discrepancy, we hypothesize that PUX10 may not be the only LD-associated protein able to bind CDC48A. CDC48A could be targeted to LDs by interaction with an unknown LD protein distinct from PUX10 and expressed in Arabidopsis seedlings but not in *N. benthamiana* leaves. Consistent with this hypothesis, we observed a lack of association between CDC48A and PUX10 levels in purified LDs at different stages of seed germination, as measured by LD proteomics (Supplemental Figure 1) and immunoblots (Figure 7A). Overall, we conclude that PUX10 is an integral LD protein promoting CDC48A association with LDs, although this targeting mechanism of CDC48A to LDs may not be the only one involved in seedlings.

PUX10 can bridge ubiquitin to CDC48A through its UBA and UBX domains

The presence of both UBX and UBA domains in PUX10 strongly suggests a role as an adaptor bridging CDC48A to the ubiquitin moiety of ubiquitinated proteins. We used a yeast three-hybrid assay to reveal the formation of a ternary complex between ubiquitin, PUX10 and CDC48A. The expression of PUX10 in a yeast strain expressing ubiquitin and CDC48A allowed yeast growth on selective medium (Figure 8A), showing that PUX10 is necessary and sufficient to bridge CDC48A to ubiquitin. The deletion of either the UBA or the UBX domain suppressed this interaction (Figure 8A), indicating that these domains are involved in PUX10 interaction with ubiquitin or CDC48A. To ensure that the UBA and UBX domains are sufficient for PUX10 interaction with its partners, we investigated the ability of these domains to bind either ubiquitin or CDC48A, using the yeast two-hybrid method. The PUX10 N-terminus region (M^{1}-S^{44}) encompassing the UBA domain (F^{11}-T^{42}, as determined on NCBI CD Search) was sufficient to bind ubiquitin but not CDC48A (Figure 8B). Conversely, the PUX10 C-terminus region (E^{398}-N^{480}) encompassing the UBX domain (E^{398}-E^{478}, as determined on NCBI CD Search) was sufficient for the specific interaction with CDC48A but did not bind ubiquitin. These two pairs of interaction, i.e., ubiquitin-UBA domain and CDC48A-UBX domain, were confirmed in both orientations of bait and target (Figure 8B).

The interaction between PUX10 and CDC48A was also demonstrated *in planta* using bimolecular fluorescence complementation. The *in vivo* formation of a stable PUX10-CDC48A complex, visualized by the emission of YFP fluorescence, occurred in LDs and chloroplast membranes of agrobacterium-inoculated *N. benthamiana* epidermal cells (Figure 8C; magnified views in the right panel). This interaction is consistent with the subcellular localizations of both PUX10 and CDC48A previously observed in Figures 5 and 6. Moreover, we confirmed *in planta* that the interaction of PUX10 with CDC48A is mediated by its UBX domain, as co-expression of YFP^N-PUX10ΔUBX and YFP^C-CDC48A resulted in significantly fewer fluorescent punctae compared to co-expression of full-length proteins (Figure 8D).

PUX10 is required for segregation of the ubiquitinated oleosins

In germinated seeds, OLEs-$K48Ub_2$ is extracted from the phospholipid monolayer surrounding LDs before reaching the cytosolic proteasome for degradation (Deruyffelaere et al., 2015). The extraction of ubiquitinated oleosins from LDs may be catalyzed by the CDC48A ATPase. Numerous studies in animals and yeast have indeed reported that CDC48 ATPases have the ability to physically disassemble ubiquitinated proteins from binding partners or cellular structures with the help of associated cofactors (Meyer et al., 2012). We thus hypothesized that PUX10 could be the cofactor promoting CDC48A activity to disassemble OLEs-$K48Ub_2$ from LDs in germinated seeds. To investigate this possibility, we analyzed the intracellular distribution of the ubiquitinated oleosins over-accumulated in *pux10-1* seedlings. Most of the OLEs-$K48Ub_2$ accumulated in *pux10-1* seedlings were present in the LD fraction, showing that *PUX10* mutation interferes with the segregation of OLEs-$K48Ub_2$ from LDs (Figure 9; Apu2 immunoblot). By contrast, accumulation of OLEs-$K48Ub_2$ due to MG132-induced proteasome blockade was recovered in the insoluble protein fraction (P2 pellet) of wild-type seedling extracts (Figure 9; Apu2 immunoblot). This result confirmed that proteasome inhibition blocks the degradation of OLEs-$K48Ub_2$ after their extraction from LDs. Extracted OLEs-$K48Ub_2$ were no longer degraded by the proteasome and consequently aggregated within the cytosol due to their hydrophobicity. We also analyzed the intracellular distribution of the two other types of ubiquitin-oleosin

conjugates, i.e., OLEs-Ub and OLEs-K63Ub$_2$. In the *pux10-1* mutant, over-accumulated OLEs-Ub and OLEs-K63Ub$_2$ were essentially associated with LDs (Figure 9; FK2 and Apu3 immunoblots), indicating that PUX10 is required for the dislocation of OLEs-Ub and OLEs-K63Ub$_2$ from LDs. MG132 did not impair the degradation of these two types of ubiquitin-oleosin conjugates, suggesting that oleosins modified by the covalent binding of a monoubiquitin or a K63-linked diubiquitin are not targeted to the UPS. In conclusion, this experiment demonstrated that PUX10 is required for the segregation of all three types of ubiquitinated oleosins from LDs, regardless of the topology of ubiquitination. It also showed that, once dislocated from the LDs to the cytosol, ubiquitinated oleosins are targeted to distinct degradation pathways according to the topology of their ubiquitin moiety. Whereas the UPS hydrolyses OLEs-K48Ub$_2$, the degradation pathways of OLEs-Ub and OLEs-K63Ub$_2$ are currently unknown.

Discussion

A significant remodeling of the LD proteome occurs during the transition from seed dormancy to postgerminative growth. In the quiescent cells of mature seeds, LDs are coated and stabilized by oleosins. When seeds germinate, oleosins are progressively degraded (Deruyffelaere et al., 2015) and replaced by LDAPs, which are the structural LD proteins recently identified in non-seed cells (Gidda et al., 2016). Why are oleosins replaced by LDAPs at the LD surface? When overexpressed in leaves, both families of proteins are able to increase the accumulation of neutral lipids and to compartmentalize them into normal-sized LDs, showing that they function similarly and as expected for structural LD proteins (Winichayakul et al., 2013; Vanhercke et al., 2014; Gidda et al., 2016). However, oleosins prevent other proteins, such as LDAPs in leaves or native LD proteins in yeast, from targeting to LDs (Jamme et al., 2013; Gidda et al., 2016). These results suggest that oleosins impair LD remodeling and maintain the organelle in a quiescent state. Therefore, the degradation of oleosins is likely required for LDs to enter the dynamic state associated with seedling growth. The present study focused on deciphering the molecular machinery controlling oleosin degradation, and thus

represents an important early step in understanding the subcellular processes involved in the transition from quiescent to dynamic LDs during germination.

Oleosins are degraded by a novel protein degradation pathway called LD-associated degradation (LDAD)

Here, we demonstrated that PUX10 is an integral LD protein that acts as an adaptor directly linking CDC48A to ubiquitin conjugates. The UBX and UBA domains of PUX10 were shown to mediate PUX10 interaction with CDC48A and ubiquitin conjugates, respectively. PUX10 is therefore the fifth Arabidopsis PUX protein shown to be a functional cofactor of CDC48A, out of 16. More importantly, PUX10 is the first PUX protein whose ubiquitinated substrates have been identified. The accumulation of ubiquitinated oleosins and the reduction of oleosin degradation observed in *pux10-1* and *pux10-2* seedlings demonstrate that ubiquitin-conjugated oleosins are specific substrates of PUX10.

We also provided evidence that CDC48A and PUX10 are part of a protein machinery segregating ubiquitinated oleosins from LDs. Our findings indicate that PUX10 is required for the extraction of all types of ubiquitinated oleosins from the LD surface into the cytosol. Given that CDC48A co-localizes and interacts with PUX10 on LDs (Figures 6 and 8), and that CDC48A belongs to a family of ubiquitous proteins known for their ability to physically disassemble ubiquitinated proteins from membranes or complexes (Bodnar and Rapoport, 2017), the role of PUX10 in this dislocation process most likely occurs by promoting the interaction of CDC48A with ubiquitinated oleosins. Intriguingly, our data revealed that PUX10 is not able to discriminate the different ubiquitin motifs conjugated to oleosins. Mutations in *PUX10* indeed blocked not only the proteasomal degradation of OLEs-K48Ub_2, but also the proteasomal-independent degradation of OLEs-K63Ub_2 and OLEs-Ub. Some yet unknown CDC48A cofactors, which selectively bind either K48Ub_2-, K63Ub_2- or Ub-conjugated oleosins, are probably required to mediate specificity for degradation pathways.

Cellular functions of CDC48A homologs in yeast and mammals are well documented, starting with their role in the selective extraction of misfolded proteins from the ER, a key step in the degradation process known as ERAD. Besides ERAD, yeast Cdc48 and

mammalian p97/VCP are also involved in dislocating proteins from the mitochondrial outer membrane, in a process termed mitochondria-associated degradation (MAD) (Xu et al., 2011; Braun and Westermann, 2017). In plants, there is no evidence of a MAD pathway to date, but several components of the ERAD process have been identified, including Arabidopsis CDC48A (Muller et al., 2005; Begue et al., 2017), uncovering similar mechanisms of ER-associated protein degradation in plants and in yeast or mammals (Muller et al., 2005; Liu and Li, 2014). An ERAD-like machinery is also associated with plastids derived by secondary endosymbiosis (called complex plastids), in secondary red algal endosymbionts such as diatoms. Contrary to ERAD and MAD, this Cdc48-containing machinery, called symbiont-specific ERAD-like machinery (SELMA), is not involved in protein degradation but is required for the transport of nuclear-encoded proteins across the periplastidial membrane of complex plastids (Agrawal et al., 2009; Lau et al., 2015). Besides the ER, mitochondria and plastids, the present study thus identifies LDs as another organelle targeted by an ERAD-like CDC48-containing machinery. Together with CDC48A, PUX10 would be a core component of this putative machinery, which we name LD-associated degradation (LDAD).

This ubiquitin- and PUX10-dependent system is the first molecular mechanism of LD protein degradation identified in plants. This pathway is distinct from the ones previously identified in mammals. The first mechanism described to control protein turnover in mammalian LDs involves ARF1 and the coat protein complex I (COPI), two components of the vesicular trafficking pathway (Soni et al., 2009; Takashima et al., 2011). The ARF1-COPI machinery associates with LDs and releases portions of the LD surface by budding nano-LDs. This budding process triggers LD-ER connections, which are used for protein relocalization (Wilfling et al., 2013). More recently, PLIN2 and PLIN3, the major LD proteins in non-adipose tissues, were shown to be degraded by chaperone-mediated autophagy (CMA), a highly selective form of autophagy (Kaushik and Cuervo, 2015). Intriguingly, although neither of these pathways is dependent on ubiquination, several mammalian LD proteins are ubiquitinated and degraded by the UPS, such as PLIN1 and PLIN2, the mammalian LD gatekeepers (Xu et al., 2005; Xu et al., 2006). Moreover, several proteins of the ubiquitination machinery are associated with LDs in

yeast and mammals (Bersuker and Olzmann, 2017), including p97/VCP/Cdc48 and the counterparts of PUX10. These latter, namely human FAF2/UBXD8 and *Saccharomyces cerevisiae* Ubx2p, can relocalize from the ER to LDs and regulate LD dynamics (Zehmer et al., 2009; Wang and Lee, 2012; Olzmann et al., 2013), besides their role in ERAD. The prominent presence of proteins related to the ubiquitin system in mammalian LDs was recently confirmed by mapping human LD proteomes using a proximity labelling strategy (Bersuker et al., 2018). Overall, these data raise the possibility that the LDAD pathway, uncovered herein in plants, might also be present in mammals and yeast. Demonstrating this hypothesis will require identifying LD-associated proteins regulated by ubiquitination and accumulated in some LDAD-deficient mutants. One candidate substrate of the putative mammalian LDAD is Apo-B100, which translocates to LDs before its proteasomal degradation by a UBXD8-dependent mechanism (Suzuki et al., 2012).

PUX10 and CDC48A discriminate subpopulations of LDs in seedlings

The comprehensive analysis of PUX10 localization revealed distinct targeting pathways during seed development and germination. While PUX10 is exclusively associated with LDs in germinating seeds and young seedlings, it shows a more complex localization pattern in developing seeds. During embryogenesis, PUX10 is mainly associated with LDs but also localizes to the ER. This dual steady-state localization to LDs and the ER was also observed by transient expression in *N. benthamiana* leaves, and previously reported for the yeast and mammalian homologs of PUX10 (Wang and Lee, 2012; Olzmann et al., 2013). The hydrophobic HP domain of PUX10 serves as a membrane anchor and is required for this dual localization. This domain may form a hairpin with arms of 15-20 residues, which are short enough for PUX10 to partition between the cytoplasmic leaflet of the ER and the LD monolayer, according to Huang and Huang (2017). The targeting patterns of PUX10 in developing and germinating seeds are consistent with the prevailing model of LD targeting for class I LD proteins (Kory et al., 2016). This model posits that class I LD proteins are co-translationally inserted into the ER membrane and transferred either directly to the nascent LDs emerging from ER subdomains, or to some mature LDs through specific ER-LD membrane bridges. In developing seeds, PUX10 is associated with the pool of LDs, suggesting its insertion

into the LD monolayer during organelle biogenesis. In the cotyledons and hypocotyl of germinated seeds, PUX10 is progressively expressed and sequentially translocated to a specific subset of LDs, possibly through ER-LD connections. The molecular machinery by which PUX10 is translocated to LDs is currently unknown. However, the translocation mechanism is probably distinct from the ARF1/COPI-mediated mechanism described in mammals (Wilfling et al., 2014), since proteins of the ARF family were not identified in the LD proteome of Arabidopsis seedlings (Pyc et al., 2017b). Unexpectedly, we observed a dramatic change of PUX10 localization during the transition between embryogenesis and seed maturation. At 12 DAF, PUX10 exclusively localizes to the chloroplast periphery, which is a localization also observed in *N. benthamiana* leaves. However, while PUX10 targeting pathways to LD monolayer and to chloroplast membranes are both functional in *N. benthamiana* epidermal cells, they are mutually exclusive and sequentially activated during seed development and germination. Thus, PUX10 partitioning between LDs and chloroplasts is subject to a developmental control, which represents a potentially important mechanism for regulating LD dynamics in seeds.

In considering the functional significance of the interaction between PUX10 and CDC48A, the prevailing hypothesis is that PUX10 serves as an anchor for targeting the cytoplasmic CDC48A to LDs. Although tantalizingly simple, this hypothesis might not represent the whole story, since the association of CDC48A with LDs is not disrupted in *pux10-1* and *pux10-2* seedlings. A similar observation was reported for Ubx2 and Cdc48 in yeast ERAD, suggesting an evolutionary-conserved functional redundancy of membrane-recruitment factors for CDC48s (Neuber et al., 2005). Thus, another LD-recruitment factor for CDC48A might exist in young seedlings, in addition to PUX10. This hypothesis can also explain the partial loss-of-function associated with PUX10 deficiency in *pux10-1* and *pux10-2* mutants. However, the putative LD-recruitment factor would only partially compensate for PUX10 deficiency as the *pux10-1* and *pux10-2* seedlings exhibit a major reduction of oleosin degradation. These results suggest that PUX10 is required to facilitate correct orientation of ubiquitinated oleosin and CDC48A for efficient substrate binding and subsequent processing, while it is not mandatory for the recruitment of CDC48A to LDs in seedlings.

One important finding of the present study is the coexistence of distinct LD subpopulations within a single cell, suggesting a functional differentiation of LDs in plants. Morphological and compositional heterogeneity within the LD pool of a single cell have been described for several years in animals and yeast, but not in plants (Wolins et al., 2005; Beller et al., 2006; Wilfling et al., 2013; Zhang et al., 2016; Thiam and Beller, 2017; Eisenberg-Bord et al., 2018). In cotton (*Gossypium hirsutum*) and Arabidopsis plants, Horn et al. (2011) reported the uneven distribution of triacylglycerol species among individual LDs isolated from seed or leaf tissues, suggesting that LD heterogeneity may also exist in plants, at least at the tissue level (Horn et al., 2011). Such a heterogeneity was proved at the cell level in the present study. PUX10 and CDC48A, which exclusively localize on a subset of LDs in seedling cotyledons and hypocotyls, are indeed determinants of a LD subpopulation in Arabidopsis. Undoubtedly, it will be interesting to characterize the difference in protein and lipid compositions between the PUX10-free and PUX10-coated LD subpopulations, and to examine if proteins and organelles involved in seed LD dynamics, such as LDAPs, LDIP, SEIPINs, SDP1 and peroxisomes, are preferentially or exclusively associated with a specific subset of LDs (Kelly et al., 2011; Cai et al., 2015; Thazar-Poulot et al., 2015; Gidda et al., 2016; Pyc et al., 2017a).

A working model of the LDAD pathway

The complete proteolysis of type I LD proteins, such as oleosins, requires unmasking of hydrophobic domains embedded in the phospholipid monolayer. Our results shed light on a mechanism able to dislocate these proteins from the LD surface. PUX10 and CDC48A are central to this mechanism. PUX10 is a LD-anchored scaffolding protein that bridges the CDC48A segregase to the substrate, i.e., ubiquitinated oleosins, to promote the dislocation of ubiquitinated oleosins from the phospholipid monolayer (Figure 10). This mechanism is reminiscent of the ERAD translocation process but localizes to LDs; we therefore propose to name it LDAD. Further characterization of the LDAD pathway will require the identification of additional proteins of the LDAD machinery, besides PUX10 and CDC48A. This includes proteins involved in pre-dislocation events, such as ubiquitin ligases, and in post-dislocation events, such as

substrate-processing cofactors controlling ubiquitin chain editing or recruiting specific proteolytic systems according to the ubiquitin mark borne by oleosins.

Methods

Plant material, germination and growth conditions

Arabidopsis thaliana seeds of the Ws and Col0 ecotypes and of the T-DNA mutant line *pux10-2* (FLAG_211E02) were obtained from the *Arabidopsis thaliana* resource center for genomics at the Institut Jean-Pierre Bourgin (http://publiclines.versailles.inra.fr/). The T-DNA mutant line *pux10-1* (SAIL_1187) was ordered from the NASC (http://arabidopsis.info). The *pux10-1* and *pux10-2* mutants are in Col0 and Ws genetic backgrounds, respectively. The Arabidopsis *ProCDC48A:YFP-CDC48A*/*Atcdc48A* line (expressing YFP-CDC48A) was kindly provided by S.Y. Bednarek (Park et al., 2008). The *pux10-1* and *pux10-2* T-DNA insertion lines were genotyped using the primers pux10_SAIL_for/ pux10_SAIL_rev and pux10_FLAG_for/ pux10_FLAG_rev, respectively (see Supplemental Table 1 for primer sequences). DNA insertion positions within *PUX10* were determined by DNA sequencing of the PCR-amplified products obtained with T-DNA-specific primers and primers on either side of the *PUX10* insertion site. The location of insertion was mapped between positions 6642476 and 6642398 of Chr4 for *pux10-1* and at position 6641494 of Chr4 for *pux10-2*. Homozygous *pux10*-1 and *pux10-2* plants were backcrossed twice to wild-type Col-0 and Ws ecotype plants, respectively. RT-PCR analyses were ultimately carried out to analyze gene expression in mutant backgrounds. The sequences of primers used for PCR amplifications are listed in Supplemental Table 1.

For the selection of Arabidopsis transgenic plants, seeds were surface-sterilized, stratified for 7 2h at 4°C in the dark and germinated on full-strength Gamborg B5 medium, pH 5.6 (Duchefa Biochemie), containing 0.8% (w/v) agar, 1% (w/v) sucrose, and the appropriate selection agent. After 14 days of selection in a growth cabinet (16-h-light/8-h-dark cycle), plantlets were transferred to compost. *Arabidopsis thaliana* wild-type and transgenic plants were grown on soil in long-day conditions (16-h-light/8-h-dark cycle) in greenhouse or growth chamber. Control seeds were grown side by side

with experimental seeds for each experiment. For biochemical analyses and imaging, seeds were cold stratified and germinated on water-imbibed paper at 25°C under continuous light, as described in Deruyffelaere et al. (2015). Seeds were collected just after stratification (imbibed seeds; 0 h of germination) or after 24–72 h of incubation at 25°C (24–72 h of germination). When indicated, seeds were germinated in water containing 100 µM MG132 (Sigma-Aldrich) or 0.1% DMSO as a solvent control.

For germination assays, seeds were incubated at 25°C, with 8 h light daily, on three sheets of absorbent paper (paper circles, Schleicher and Schuell) wetted with distilled water. Germination was scored daily based on radicle emergence.

Agrobacterium-mediated transient expression in *Nicotiana benthamiana* leaves

Agrobacterium tumefaciens strain C58C1pMP90 was transformed by electroporation with pMDC32-mCherry-PUX10, pGWB6-GFP-PUX10, pGWB6-GFP-PUX10-ΔUBX, pGWB6-GFP-PUX10c-ΔHP, pMDC32-mCherry-CDC48A or pB7WGF2-GFP-OLE1 binary plasmid. After overnight culture at 28°C in LB medium containing antibiotics (rifampicin 50 µg/mL, gentamycin 50 µg/mL, kanamycin 50 µg/mL), agrobacteria were centrifuged and resuspended in infiltration buffer (10 mM $MgCl_2$, 10 mM 2-(N-morpholino)ethanesulfonic acid (MES) pH 5.7) at 0.1 OD_{600} for each construct. Agrobacteria infiltration was performed at the abaxial face of leaves from 4-week-old plants using a syringe, 2 to 3 d before imaging. When indicated, *N. benthamiana* plants expressing an ER resident red fluorescent protein (RFP-ER) were used instead of wild-type plants (Martin et al., 2009).

Agrobacterium-mediated stable transformation and selection of transgenic lines

Arabidopsis mutant *pux10-1* plants were transformed by the floral dip method with the *Agrobacterium tumefaciens* strain C58C1pMP90 containing the pGWB4-ProPUX10:PUX10-GFP or pGWB16-ProPUX10:PUX10-myc binary vector (Clough and Bent, 1998). Hygromycin-resistant transgenic plants were obtained and were self-pollinated to obtain F2 progenies. Seeds from homozygous F2 plants were used for visualization of the fluorescent protein and for immunoblot analysis.

Plasmid constructions

Plant and yeast expression vectors were constructed using Gateway cloning technology as described in the Gateway technology instruction manual (Invitrogen, http://www.lifetechnologies.com). To generate entry vectors with full-length or truncated versions of *PUX10* and full-length *OLE1*, *PUX10* cDNA or gene and *OLE1* cDNA were amplified by PCR using attB-flanked primers and the Phusion High-Fidelity DNA Polymerase (Thermo Fisher Scientific) before BP clonase recombination into the pDONR207 vector (Invitrogen). The pENTR-PUX10c-ΔHP plasmid was generated by mutagenesis of pENTR-PUX10-stop using a Q5 site-directed Mutagenesis Kit (Clontech) to remove the transmembrane-coding region. Various expression vectors were obtained by LR reaction between these entry vectors and a set of Gateway-based destination vectors. The destination vectors used in this study are as follows: pGWB6 for 35S-driven N-terminal GFP fusions and pGWB4 for C-terminal GFP fusions w/o promoter (Nakagawa et al., 2007); pB7WGF2 for 35S-driven N-terminal GFP fusions (Karimi et al., 2002); pDEST-GADT7 and pDEST-GBKT7 for yeast two-hybrid interaction studies (Rossignol et al., 2007); pARC351 for yeast three-hybrid interaction studies (Ferrario et al., 2003); pBIFP2 and pBIFP3 for bimolecular fluorescent complementation experiments (Azimzadeh et al., 2008); and pMDC32-mCherry for 35S-driven N-terminal mCherry fusions. The latter binary vector was constructed by inserting the mCherry gene, amplified using mCherry_Nter and mCherry_Cter primers, between the *Kpn*I and *Asc*I sites of pMDC32 (Curtis and Grossniklaus, 2003), and was kindly provided by Valérie Gaudin and Nathalie Simoncello (INRA de Versailles, France). Primer sequences are listed in Supplemental Table 1. More detailed information about plasmid construction is available in Supplemental Table 2. All constructs were confirmed by DNA sequencing.

LD isolation

Using a glass-glass conical tissue grinder, dry or germinated seeds were ground in seed homogenization buffer (SH buffer; 100 mM HEPES pH 7.5, 500 mM sorbitol, 150 mM KCl, 1 mM $MgCl_2$, 1 mM EDTA) containing protease inhibitors (complete mini EDTA-free, Roche) and 10 mM N-ethylmaleimide to prevent deubiquitinase activity. LDs were isolated from homogenized seeds/seedlings by ultracentrifugation on a

discontinuous iodixanol density gradient, and recovered in the floating fraction, as described in Deruyffelaere et al. (2015). To analyze the protein association to LDs, freshly isolated LDs were diluted into 100 mM Na carbonate containing 8 M urea (pH 10), or alternatively, into SH buffer. Samples were incubated at 4°C for 30 min on a rotating agitator. Washed LDs were re-isolated by ultracentrifugation on a discontinuous iodixanol density gradient, according to the same protocol as used for the first isolation.

Protein analysis by SDS-PAGE and immunoblotting

Total seed/seedling protein extracts were prepared by direct homogenization in 2X NuPAGE LDS Sample Buffer (Thermo Fisher Scientific) containing 0.1 M dithiothreitol, as described in Deruyffelaere (2015). LD proteins were precipitated with cold acetone containing 10% (v/v) trichloroacetic acid and solubilized in 2X LDS buffer containing 200 mM Tris base and 0.1 M dithiothreitol. Protein extracts were incubated at 37°C for 10 min, separated by electrophoresis in NuPAGE gels with MOPS SDS running buffer, and blotted in NuPAGE transfer buffer (Thermo Fisher Scientific). For anti-PUX10 or -OLEs immunoblot, proteins were transferred to polyvinylidene difluoride membranes (Immobilon-P 0.45 mm, Millipore). For anti-CDC48A immunoblot, proteins were blotted onto nitrocellulose membrane (BAS-85, Schleicher and Schuell). Saturation and incubation with antibodies were carried out according to D'Andrea et al. (2007). Rabbit anti-oleosin sera were used as previously described (D'Andrea et al., 2007). Rabbit antibodies recognizing polyubiquitin chains linked at Lys48 (clone Apu2, cat. 05-1307, lot 2840426) or Lys63 (clone Apu3, cat. 05-1308, lot 2923061) and mouse antibody against ubiquitinated proteins (clone FK2, cat. 04-263, lot 2475581) were obtained from Millipore and used at 1:1,000 dilution for Apu2 and FK2 and at 1:500 dilution for Apu3. Chicken antiserum specific to Arabidopsis CDC48A was kindly given by S.Y. Bednarek and used according to Park et al. (2008). Luminescence from peroxidase activity, revealed using Super Signal West Dura Extended Duration Substrate (Pierce), was recorded using a LAS-3000 imaging system and quantified with MultiGauge software, both from Fujifilm. After immunodetection, proteins were stained on membranes with amido black 10B (Gershoni and Palade, 1982) to control protein loading.

Fatty acid analysis by gas chromatography

Total fatty acid content and composition of mature or germinated seeds were determined by direct transmethylation followed by gas chromatography with flame ionization detection (GC-FID) as previously described (Browse et al., 1986), with the minor modifications described in Deruyffelaere et al. (2015). For each batch of seeds, FA analysis was performed in triplicate or quadruplicate on 30 or 100 seeds/seedlings.

Confocal Laser Scanning Microscopy (CSLM)

For visualizing LDs, *Arabidopsis* seedlings were incubated in HCS LipidTOX™ Deep Red Neutral Lipid Stain (ThermoFisher Scientific, 500-fold dilution in water) for 30 min before imaging. *Arabidopsis* seeds/seedlings and agro-infiltrated *N. benthamiana* leaves were imaged with a Leica SP8 confocal laser scanning microscope. GFP and chloroplast autofluorescence were excited with the 488-nm line of an argon laser, mCherry and RFP with a 561-nm diode laser, YFP was excited with the 514-nm line of an argon laser, and LipidTOX Deep Red with a 633-nm helium/neon laser. Fluorescence emission was detected between 495–510 nm for GFP, 522-550 nm for YFP, 600–625 nm for mCherry and RFP, and 637-650 for LipidTOX Deep Red. Chloroplast autofluorescence was imaged between 670-700 nm. For multi-labelling studies, detection was performed in a sequential line-scanning mode. The apparent diameter of LDs observed by CLSM and bright-field microscopy was estimated using ImageJ software (http://rsbweb.nih.gov/ij/), by manually drawing the diameter using the "line" tool and measuring it with the "measure" function of the software.

Protein-protein interaction studies in yeast and *in planta*

Yeast interaction assays were carried out using the Matchmaker GAL4 two-hybrid system 3 from Clontech, according to protocols described in the Yeast Protocols Handbook (Clontech). For yeast two-hybrid (Y2H) analyses, pGADT7- and pGBKT7-derived plasmids were introduced by lithium acetate transformation into PJ69-4A and PJ69-4α strains, respectively. For yeast three-hybrid (Y3H) analyses, PJ69-4A clone transformed with pGADT7-CDC48A was re-transformed with the pARC351-derived vectors. Transformed yeasts were selected on SD medium lacking specific amino-acids, according to the auxotrophy genes carried by the cloning vectors. After appropriate mating between PJ69-4A and PJ69-4 α clones, diploid cells were selected on SD

medium lacking leucine and tryptophane (SD-LW) for Y2H assays, and on SD medium lacking leucine, tryptophane and uracyl (SD-LWU) for Y3H assays. Protein interactions were assayed by growing diploid cells on selective medium lacking leucine, tryptophane and histidine (SD-LWH) for Y2H assays, and on medium lacking leucine, tryptophane, uracyl and histidine (SD-LWUH) for Y3H assays.

Protein interactions were tested *in planta* using a bimolecular fluorescence complementation (BiFC) assay. Leaf epidermal cells of *N. benthamiana* plants expressing ER-RFP were transiently co-transformed with agrobacteria harboring pBiFP3-YFP^{C}-CDC48A (Gallois et al., 2013) and pBiFP2-YFP^{N}-PUX10 or pBiFP2-YFP^{N}-PUX10-ΔUBX (Supplemental Table 2). Two days after infiltration, YFP fluorescence was imaged by CLSM. The interaction between the MADS box transcription factors DEFICIENS and GLOBOSA was used as a positive control and carried out by co-infiltration with the pBIFP2-DEF and pBIFP3-GLO constructs (Ferrario et al., 2003). For BiFC quantification, fluorescent punctae were numbered in several areas of transformed epidermal cells, identical in size and imaged using the same CLSM acquisition settings, as previously described (Stefano et al., 2015).

Accession numbers

The Arabidopsis Genome Initiative locus identifiers for the genes mentioned in this article are *PUX10* (At4g10790), *PUX7* (At1g14570), *CDC48A* (At3g09840), *EF1*α (At5g60390), *OLE1* (At4g25140), *OLE2* (At5g40420).

Protein sequence data for the alignment of PUX10 can be found in the UniProt data library under accession numbers Q9M0N1(PUX10), Q94JZ8 (PUX7), F4JPR7 (PUX8), Q4V3D3 (PUX9), Q9ZW74 (PUX11), Q9LUG7 (PUX12), Q9C5G7 (PUX13), P0DKI4 (PUX14), Q94HV8 (PUX15), P0DKI5 (PUX16), Q9UNN5 (human FAF1), Q96CS3 (human FAF2/UBXD8), Q04228 (*S. cerevisiae* Ubx2p), and Q12229 (*S. cerevisiae* Ubx3p).

Supplemental Data

Supplemental Figure 1. PUX10 and CDC48A peptides identified in LD proteins by shotgun proteomics.

Supplemental Figure 2. Protein sequence alignment of PUX10 homologs in yeast, human and Arabidopsis, showing functional domains.

Supplemental Figure 3. Phylogenetic diagram of several *A. thaliana* PUXs (including PUX10), human FAF1 and FAF2/UBXD8, and *S. cerevisiae* Ubx2p and Ubx3p.

Supplemental Figure 4. Effect of PUX10 mutation on seed maturation and germination.

Supplemental Figure 5. Similar localization of GFP-PUX10 in post-germinated seeds of three independent stable Arabidopsis *ProPUX10:PUX10-GFP*/*pux10-1* transgenic lines (#5, #7 and #12).

Supplemental Table 1. Primers used in this study.

Supplemental Table 2. Constructs used in this study.

Supplemental Data Set 1. PUX10 and CDC48A peptides identified from LD proteins isolated from seeds and young seedlings.

Supplemental Data Set 2. Alignments used to generate the phylogeny shown in Supplemental Figure 3.

Supplemental Movie 1. PUX10-labeled LDs are moving along ER strands.

Supplemental Movie Legend.

Acknowledgments

We thank Olivier Grandjean from the Imaging and Cytology platform of IJPB for assistance with confocal microscopy and technical support for the BiFC experiments. We are grateful to Patrick Grillot for taking care of the plants. We also thank Sebastian Bednarek for providing the Arabidopsis line expressing YFP-CDC48A and the antiserum specific to CDC48A, and Valérie Gaudin, Nathalie Simoncello, Hakim Mireau and

Bertrand Dubreucq for plasmid gifts. We are grateful to Philippe Guerche, Olivier Lamotte, Loïc Rajjou, Elodie Akary and Marine Froissard for helpful discussion. Aline Ballot, Laura Doucerain, and Antoine Moniot are acknowledged for participating in the experiments during their internship.

The IJPB benefits from the support of the LabEx Saclay Plant Sciences-SPS (ANR-10-LABX-0040-SPS).

Author Contributions

S.D. conceived the research plan, designed experiments, performed experiments (cloning, transgenic construction, imaging), analyzed data, and wrote the first draft of the manuscript. C.D. conducted most of the biochemical experiments and plant production/selection. Z.P. and I.B. conducted biochemical experiments and plant production/selection. J.L.G. and S.D. designed and performed Y2H and BiFC experiments. B.C. conducted germination assays. J.L.C. produced the GFP-OLE1 construct. J.L.C., I.B., J.L.G., Z.P., T.C., and S.D. read and edited the manuscript.

References

Agrawal, S., van Dooren, G.G., Beatty, W.L., and Striepen, B. (2009). Genetic Evidence that an Endosymbiont-derived Endoplasmic Reticulum-associated Protein Degradation (ERAD) System Functions in Import of Apicoplast Proteins. J. Biol. Chem. **284,** 33683-33691.

Arrese, E.L., Saudale, F.Z., and Soulages, J.L. (2014). Lipid Droplets as Signaling Platforms Linking Metabolic and Cellular Functions. Lipid Insights **7,** 7-16.

Azimzadeh, J., Nacry, P., Christodoulidou, A., Drevensek, S., Camilleri, C., Amiour, N., Parcy, F., Pastuglia, M., and Bouchez, D. (2008). Arabidopsis TONNEAU1 proteins are essential for preprophase band formation and interact with centrin. Plant Cell **20,** 2146-2159.

Barthelme, D., and Sauer, R.T. (2016). Origin and Functional Evolution of the Cdc48/p97/VCP AAA+ Protein Unfolding and Remodeling Machine. J Mol Biol **428,** 1861-1869.

Baud, S., Boutin, J.-P., Miquel, M., Lepiniec, L., and Rochat, C. (2002). An integrated overview of seed development in Arabidopsis thaliana ecotype WS. Plant Physiology and Biochemistry **40,** 151-160.

Beaudoin, F., and Napier, J.A. (2002). Targeting and membrane-insertion of a sunflower oleosin in vitro and in Saccharomyces cerevisiae: the central hydrophobic domain contains more than one signal sequence, and directs oleosin insertion into the endoplasmic reticulum membrane using a signal anchor sequence mechanism. Planta **215,** 293-303.

Begue, H., Jeandroz, S., Blanchard, C., Wendehenne, D., and Rosnoblet, C. (2017). Structure and functions of the chaperone-like p97/CDC48 in plants. Biochim Biophys Acta **1861,** 3053-3060.

Beller, M., Riedel, D., Jansch, L., Dieterich, G., Wehland, J., Jackle, H., and Kuhnlein, R.P. (2006). Characterization of the Drosophila lipid droplet subproteome. Mol Cell Proteomics **5,** 1082-1094.

Bersuker, K., and Olzmann, J.A. (2017). Establishing the lipid droplet proteome: Mechanisms of lipid droplet protein targeting and degradation. Biochimica et Biophysica Acta (BBA) - Molecular and Cell Biology of Lipids **1862,** 1166-1177.

Bersuker, K., Peterson, C.W.H., To, M., Sahl, S.J., Savikhin, V., Grossman, E.A., Nomura, D.K., and Olzmann, J.A. (2018). A Proximity Labeling Strategy Provides Insights into the Composition and Dynamics of Lipid Droplet Proteomes. Developmental Cell **44,** 97-112.e117.

Bodnar, N., and Rapoport, T. (2017). Toward an understanding of the Cdc48/p97 ATPase. F1000Research **6,** 1318.

Brasaemle, D.L., Rubin, B., Harten, I.A., Gruia-Gray, J., Kimmel, A.R., and Londos, C. (2000). Perilipin A increases triacylglycerol storage by decreasing the rate of triacylglycerol hydrolysis. J Biol Chem **275,** 38486-38493.

Braun, R.J., and Westermann, B. (2017). With the Help of MOM: Mitochondrial Contributions to Cellular Quality Control. Trends Cell Biol **27,** 441-452.

Browse, J., McCourt, P.J., and Somerville, C.R. (1986). Fatty acid composition of leaf lipids determined after combined digestion and fatty acid methyl ester formation from fresh tissue. Anal Biochem **152,** 141-145.

Cai, Y., Goodman, J.M., Pyc, M., Mullen, R.T., Dyer, J.M., and Chapman, K.D. (2015). Arabidopsis SEIPIN Proteins Modulate Triacylglycerol Accumulation and Influence Lipid Droplet Proliferation. The Plant Cell **27,** 2616-2636.

Chapman, K.D., and Trelease, R.N. (1991). Acquisition of membrane lipids by differentiating glyoxysomes: role of lipid bodies. The Journal of Cell Biology **115,** 995-1007.

Chapman, K.D., Dyer, J.M., and Mullen, R.T. (2012). Biogenesis and functions of lipid droplets in plants: Thematic Review Series: Lipid Droplet Synthesis and Metabolism: from Yeast to Man. J Lipid Res **53,** 215-226.

Clough, S.J., and Bent, A.F. (1998). Floral dip: a simplified method for Agrobacterium-mediated transformation of Arabidopsis thaliana. Plant J **16,** 735-743.

Curtis, M.D., and Grossniklaus, U. (2003). A gateway cloning vector set for high-throughput functional analysis of genes in planta. Plant Physiol **133,** 462-469.

D'Andrea, S. (2015). Lipid droplet mobilization: The different ways to loosen the purse strings. Biochimie.

D'Andrea, S., Jolivet, P., Boulard, C., Larre, C., Froissard, M., and Chardot, T. (2007). Selective one-step extraction of Arabidopsis thaliana seed oleosins using organic solvents. J Agric Food Chem **55,** 10008-10015.

Deruyffelaere, C., Bouchez, I., Morin, H., Guillot, A., Miquel, M., Froissard, M., Chardot, T., and D'Andrea, S. (2015). Ubiquitin-Mediated Proteasomal Degradation of Oleosins is Involved in Oil Body Mobilization During Post-Germinative Seedling Growth in Arabidopsis. Plant Cell Physiol. **56,** 1374-1387.

Eisenberg-Bord, M., Mari, M., Weill, U., Rosenfeld-Gur, E., Moldavski, O., Castro, I.G., Soni, K.G., Harpaz, N., Levine, T.P., Futerman, A.H., Reggiori, F., Bankaitis, V.A., Schuldiner, M., and Bohnert, M. (2018). Identification of seipin-linked factors that act as determinants of a lipid droplet subpopulation. The Journal of Cell Biology **217,** 269-282.

Ferrario, S., Immink, R.G., Shchennikova, A., Busscher-Lange, J., and Angenent, G.C. (2003). The MADS box gene FBP2 is required for SEPALLATA function in petunia. Plant Cell **15,** 914-925.

Gallois, J.L., Drouaud, J., Lecureuil, A., Guyon-Debast, A., Bonhomme, S., and Guerche, P. (2013). Functional characterization of the plant ubiquitin regulatory X (UBX) domain-containing protein AtPUX7 in Arabidopsis thaliana. Gene **526,** 299-308.

Gershoni, J.M., and Palade, G.E. (1982). Electrophoretic transfer of proteins from sodium dodecyl sulfate-polyacrylamide gels to a positively charged membrane filter. Analytical Biochemistry **124,** 396-405.

Gidda, S.K., Park, S., Pyc, M., Yurchenko, O., Cai, Y., Wu, P., Andrews, D.W., Chapman, K.D., Dyer, J.M., and Mullen, R.T. (2016). Lipid Droplet-Associated Proteins (LDAPs) Are Required for the Dynamic Regulation of Neutral Lipid Compartmentation in Plant Cells. Plant Physiology **170,** 2052-2071.

Gidda, S.K., Watt, S., Collins-Silva, J., Kilaru, A., Arondel, V., Yurchenko, O., Horn, P.J., James, C.N., Shintani, D., Ohlrogge, J.B., Chapman, K.D., Mullen, R.T., and Dyer, J.M. (2013). Lipid droplet-associated proteins (LDAPs) are involved in the compartmentalization of lipophilic compounds in plant cells. Plant Signal Behav **8,** e27141.

Goold, H., Beisson, F., Peltier, G., and Li-Beisson, Y. (2015). Microalgal lipid droplets: composition, diversity, biogenesis and functions. Plant Cell Rep **34,** 545-555.

Horn, P.J., Ledbetter, N.R., James, C.N., Hoffman, W.D., Case, C.R., Verbeck, G.F., and Chapman, K.D. (2011). Visualization of Lipid Droplet Composition by Direct Organelle Mass Spectrometry. J. Biol. Chem. **286,** 3298-3306.

Horn, P.J., James, C.N., Gidda, S.K., Kilaru, A., Dyer, J.M., Mullen, R.T., Ohlrogge, J.B., and Chapman, K.D. (2013). Identification of a new class of lipid droplet-associated proteins in plants. Plant Physiol **162,** 1926-1936.

Hsiao, E.S., and Tzen, J.T. (2011). Ubiquitination of oleosin-H and caleosin in sesame oil bodies after seed germination. Plant Physiol Biochem **49,** 77-81.

Huang, A.H.C. (2018). Plant Lipid Droplets and Their Associated Proteins: Potential for Rapid Advances. Plant Physiology **176,** 1894-1918.

Huang, C.Y., and Huang, A.H.C. (2017). Unique Motifs and Length of Hairpin in Oleosin Target the Cytosolic Side of Endoplasmic Reticulum and Budding Lipid Droplet. Plant Physiol **174,** 2248-2260.

Huang, M.-D., and Huang, A.H.C. (2015). Bioinformatics Reveal Five Lineages of Oleosins and the Mechanism of Lineage Evolution Related to Structure/Function from Green Algae to Seed Plants. Plant Physiology **169,** 453-470.

Hurley, James H., Lee, S., and Prag, G. (2006). Ubiquitin-binding domains. Biochemical Journal **399,** 361-372.

Jamme, F., Vindigni, J.D., Mechin, V., Cherifi, T., Chardot, T., and Froissard, M. (2013). Single cell synchrotron FT-IR microspectroscopy reveals a link between neutral lipid and storage carbohydrate fluxes in S. cerevisiae. PLoS One **8,** e74421.

Jentsch, S., and Rumpf, S. (2007). Cdc48 (p97): a "molecular gearbox" in the ubiquitin pathway? Trends Biochem Sci **32,** 6-11.

Jolivet, P., Ayme, L., Giuliani, A., Wien, F., Chardot, T., and Gohon, Y. (2017). Structural proteomics: Topology and relative accessibility of plant lipid droplet associated proteins. Journal of proteomics **169,** 87-98.

Karimi, M., Inzé, D., and Depicker, A. (2002). GATEWAY vectors for Agrobacterium-mediated plant transformation. Trends in Plant Science **7,** 193-195.

Kaushik, S., and Cuervo, A.M. (2015). Degradation of lipid droplet-associated proteins by chaperone-mediated autophagy facilitates lipolysis. Nat Cell Biol **17,** 759-770.

Kelly, A.A., Quettier, A.L., Shaw, E., and Eastmond, P.J. (2011). Seed storage oil mobilization is important but not essential for germination or seedling establishment in Arabidopsis. Plant Physiol **157,** 866-875.

Kim, E.Y., Park, K.Y., Seo, Y.S., and Kim, W.T. (2016). Arabidopsis Small Rubber Particle Protein Homolog SRPs Play Dual Roles as Positive Factors for Tissue Growth and Development and in Drought Stress Responses. Plant Physiology **170,** 2494-2510.

Kory, N., Farese, R.V., Jr., and Walther, T.C. (2016). Targeting Fat: Mechanisms of Protein Localization to Lipid Droplets. Trends Cell Biol **26,** 535-546.

Lau, J.B., Stork, S., Moog, D., Sommer, M.S., and Maier, U.G. (2015). N-terminal lysines are essential for protein translocation via a modified ERAD system in complex plastids. Molecular Microbiology **96,** 609-620.

Lee, J.N., Kim, H., Yao, H., Chen, Y., Weng, K., and Ye, J. (2010). Identification of Ubxd8 protein as a sensor for unsaturated fatty acids and regulator of triglyceride synthesis. Proc Natl Acad Sci U S A **107,** 21424-21429.

Liu, Y., and Li, J. (2014). Endoplasmic reticulum-mediated protein quality control in Arabidopsis. Front Plant Sci **5,** 162.

Martin, K., Kopperud, K., Chakrabarty, R., Banerjee, R., Brooks, R., and Goodin, M.M. (2009). Transient expression in Nicotiana benthamiana fluorescent marker lines provides enhanced definition of protein localization, movement and interactions in planta. Plant J **59,** 150-162.

Meyer, H., Bug, M., and Bremer, S. (2012). Emerging functions of the VCP/p97 AAA-ATPase in the ubiquitin system. Nat Cell Biol **14,** 117-123.

Miquel, M., Trigui, G., d'Andréa, S., Kelemen, Z., Baud, S.b., Berger, A., Deruyffelaere, C., Trubuil, A., Lepiniec, L., and Dubreucq, B. (2014). Specialization of Oleosins in Oil Body Dynamics during Seed Development in Arabidopsis Seeds. Plant Physiology **164,** 1866-1878.

Muller, J., Piffanelli, P., Devoto, A., Miklis, M., Elliott, C., Ortmann, B., Schulze-Lefert, P., and Panstruga, R. (2005). Conserved ERAD-like quality control of a plant polytopic membrane protein. Plant Cell **17,** 149-163.

Murphy, D.J. (2012). The dynamic roles of intracellular lipid droplets: from archaea to mammals. Protoplasma **249,** 541-585.

Nakagawa, T., Kurose, T., Hino, T., Tanaka, K., Kawamukai, M., Niwa, Y., Toyooka, K., Matsuoka, K., Jinbo, T., and Kimura, T. (2007). Development of series of gateway binary vectors, pGWBs, for realizing efficient construction of fusion genes for plant transformation. J Biosci Bioeng **104,** 34-41.

Neuber, O., Jarosch, E., Volkwein, C., Walter, J., and Sommer, T. (2005). Ubx2 links the Cdc48 complex to ER-associated protein degradation. Nature Cell Biology **7,** 993.

Olzmann, J.A., Richter, C.M., and Kopito, R.R. (2013). Spatial regulation of UBXD8 and p97/VCP controls ATGL-mediated lipid droplet turnover. Proc Natl Acad Sci U S A **110,** 1345-1350.

Park, S., Rancour, D.M., and Bednarek, S.Y. (2007). Protein domain-domain interactions and requirements for the negative regulation of Arabidopsis CDC48/p97 by the plant ubiquitin regulatory X (UBX) domain-containing protein, PUX1. J Biol Chem **282,** 5217-5224.

Park, S., Rancour, D.M., and Bednarek, S.Y. (2008). In Planta Analysis of the Cell Cycle-Dependent Localization of AtCDC48A and Its Critical Roles in Cell Division, Expansion, and Differentiation. Plant Physiology **148,** 246-258.

Pyc, M., Cai, Y., Greer, M.S., Yurchenko, O., Chapman, K.D., Dyer, J.M., and Mullen, R.T. (2017a). Turning Over a New Leaf in Lipid Droplet Biology. Trends in Plant Science **22,** 596-609.

Pyc, M., Cai, Y., Gidda, S.K., Yurchenko, O., Park, S., Kretzschmar, F.K., Ischebeck, T., Valerius, O., Braus, G.H., Chapman, K.D., Dyer, J.M., and Mullen, R.T. (2017b). Arabidopsis lipid droplet-

associated protein (LDAP) – interacting protein (LDIP) influences lipid droplet size and neutral lipid homeostasis in both leaves and seeds. The Plant Journal **92,** 1182-1201.

Rancour, D.M., Dickey, C.E., Park, S., and Bednarek, S.Y. (2002). Characterization of AtCDC48. Evidence for Multiple Membrane Fusion Mechanisms at the Plane of Cell Division in Plants. Plant Physiology **130,** 1241-1253.

Rancour, D.M., Park, S., Knight, S.D., and Bednarek, S.Y. (2004). Plant UBX Domain-containing Protein 1, PUX1, Regulates the Oligomeric Structure and Activity of Arabidopsis CDC48. J. Biol. Chem. **279,** 54264-54274.

Rossignol, P., Collier, S., Bush, M., Shaw, P., and Doonan, J.H. (2007). Arabidopsis POT1A interacts with TERT-V(I8), an N-terminal splicing variant of telomerase. J Cell Sci **120,** 3678-3687.

Roux, E., Baumberger, S., Axelos, M.A., and Chardot, T. (2004). Oleosins of Arabidopsis thaliana: expression in Escherichia coli, purification, and functional properties. J Agric Food Chem **52,** 5245-5249.

Rowe, E.R., Mimmack, M.L., Barbosa, A.D., Haider, A., Isaac, I., Ouberai, M.M., Thiam, A.R., Patel, S., Saudek, V., Siniossoglou, S., and Savage, D.B. (2016). Conserved Amphipathic Helices Mediate Lipid Droplet Targeting of Perilipins 1-3. J Biol Chem **291,** 6664-6678.

Schmidt, M.A., and Herman, E.M. (2008). Suppression of soybean oleosin produces micro-oil bodies that aggregate into oil body/ER complexes. Mol Plant **1,** 910-924.

Siloto, R.M., Findlay, K., Lopez-Villalobos, A., Yeung, E.C., Nykiforuk, C.L., and Moloney, M.M. (2006). The accumulation of oleosins determines the size of seed oilbodies in Arabidopsis. Plant Cell **18,** 1961-1974.

Soni, K.G., Mardones, G.A., Sougrat, R., Smirnova, E., Jackson, C.L., and Bonifacino, J.S. (2009). Coatomer-dependent protein delivery to lipid droplets. Journal of Cell Science **122,** 1834-1841.

Stefano, G., Renna, L., and Brandizzi, F. (2015). BiFC for protein-protein interactions and protein topology: discussing an integrative approach for an old technique. Methods in molecular biology **1242,** 173-182.

Suzuki, M., Otsuka, T., Ohsaki, Y., Cheng, J., Taniguchi, T., Hashimoto, H., Taniguchi, H., and Fujimoto, T. (2012). Derlin-1 and UBXD8 are engaged in dislocation and degradation of lipidated ApoB-100 at lipid droplets. Mol Biol Cell **23,** 800-810.

Sztalryd, C., and Brasaemle, D.L. (2017). The perilipin family of lipid droplet proteins: Gatekeepers of intracellular lipolysis. Biochimica et Biophysica Acta (BBA) - Molecular and Cell Biology of Lipids **1862,** 1221-1232.

Takashima, K., Saitoh, A., Hirose, S., Nakai, W., Kondo, Y., Takasu, Y., Kakeya, H., Shin, H.W., and Nakayama, K. (2011). GBF1-Arf-COPI-ArfGAP-mediated Golgi-to-ER transport involved in regulation of lipid homeostasis. Cell Struct Funct **36,** 223-235.

Thazar-Poulot, N., Miquel, M., Fobis-Loisy, I., and Gaude, T. (2015). Peroxisome extensions deliver the Arabidopsis SDP1 lipase to oil bodies. Proc Natl Acad Sci U S A **112,** 4158-4163.

Thiam, A.R., and Beller, M. (2017). The why, when and how of lipid droplet diversity. J Cell Sci **130,** 315-324.

Thiam, A.R., Farese, R.V., Jr., and Walther, T.C. (2013). The biophysics and cell biology of lipid droplets. Nat Rev Mol Cell Biol **14,** 775-786.

Vanhercke, T., El Tahchy, A., Liu, Q., Zhou, X.-R., Shrestha, P., Divi, U.K., Ral, J.-P., Mansour, M.P., Nichols, P.D., James, C.N., Horn, P.J., Chapman, K.D., Beaudoin, F., Ruiz-López, N., Larkin, P.J., de Feyter, R.C., Singh, S.P., and Petrie, J.R. (2014). Metabolic engineering of biomass for high energy density: oilseed-like triacylglycerol yields from plant leaves. Plant Biotechnology Journal **12,** 231-239.

Wang, C.-W., and Lee, S.-C. (2012). The ubiquitin-like (UBX)-domain-containing protein Ubx2/Ubxd8 regulates lipid droplet homeostasis. Journal of Cell Science **125,** 2930-2939.

Welte, M.A., and Gould, A.P. (2017). Lipid droplet functions beyond energy storage. Biochimica et Biophysica Acta (BBA) - Molecular and Cell Biology of Lipids **1862,** 1260-1272.

Wilfling, F., Thiam, A.R., Olarte, M.J., Wang, J., Beck, R., Gould, T.J., Allgeyer, E.S., Pincet, F., Bewersdorf, J., Farese, R.V., Jr., and Walther, T.C. (2014). Arf1/COPI machinery acts directly on lipid droplets and enables their connection to the ER for protein targeting. Elife **3,** e01607.

Wilfling, F., Wang, H., Haas, J.T., Krahmer, N., Gould, T.J., Uchida, A., Cheng, J.X., Graham, M., Christiano, R., Frohlich, F., Liu, X., Buhman, K.K., Coleman, R.A., Bewersdorf, J., Farese, R.V., Jr., and Walther, T.C. (2013). Triacylglycerol synthesis enzymes mediate lipid droplet growth by relocalizing from the ER to lipid droplets. Dev Cell **24,** 384-399.

Winichayakul, S., Scott, R.W., Roldan, M., Hatier, J.-H.B., Livingston, S., Cookson, R., Curran, A.C., and Roberts, N.J. (2013). In Vivo Packaging of Triacylglycerols Enhances Arabidopsis Leaf Biomass and Energy Density. Plant Physiology **162,** 626-639.

Wolins, N.E., Quaynor, B.K., Skinner, J.R., Schoenfish, M.J., Tzekov, A., and Bickel, P.E. (2005). S3-12, Adipophilin, and TIP47 Package Lipid in Adipocytes. J. Biol. Chem. **280,** 19146-19155.

Xu, G., Sztalryd, C., and Londos, C. (2006). Degradation of perilipin is mediated through ubiquitination-proteasome pathway. Biochimica et Biophysica Acta (BBA) - Molecular and Cell Biology of Lipids **1761,** 83-90.

Xu, G., Sztalryd, C., Lu, X., Tansey, J.T., Gan, J., Dorward, H., Kimmel, A.R., and Londos, C. (2005). Post-translational regulation of adipose differentiation-related protein by the ubiquitin/proteasome pathway. J Biol Chem **280,** 42841-42847.

Xu, S., Peng, G., Wang, Y., Fang, S., and Karbowski, M. (2011). The AAA-ATPase p97 is essential for outer mitochondrial membrane protein turnover. Mol Biol Cell **22,** 291-300.

Zehmer, J.K., Bartz, R., Bisel, B., Liu, P., Seemann, J., and Anderson, R.G. (2009). Targeting sequences of UBXD8 and AAM-B reveal that the ER has a direct role in the emergence and regression of lipid droplets. J Cell Sci **122,** 3694-3702.

Zhang, S., Wang, Y., Cui, L., Deng, Y., Xu, S., Yu, J., Cichello, S., Serrero, G., Ying, Y., and Liu, P. (2016). Morphologically and Functionally Distinct Lipid Droplet Subpopulations. Scientific Reports **6,** 29539.

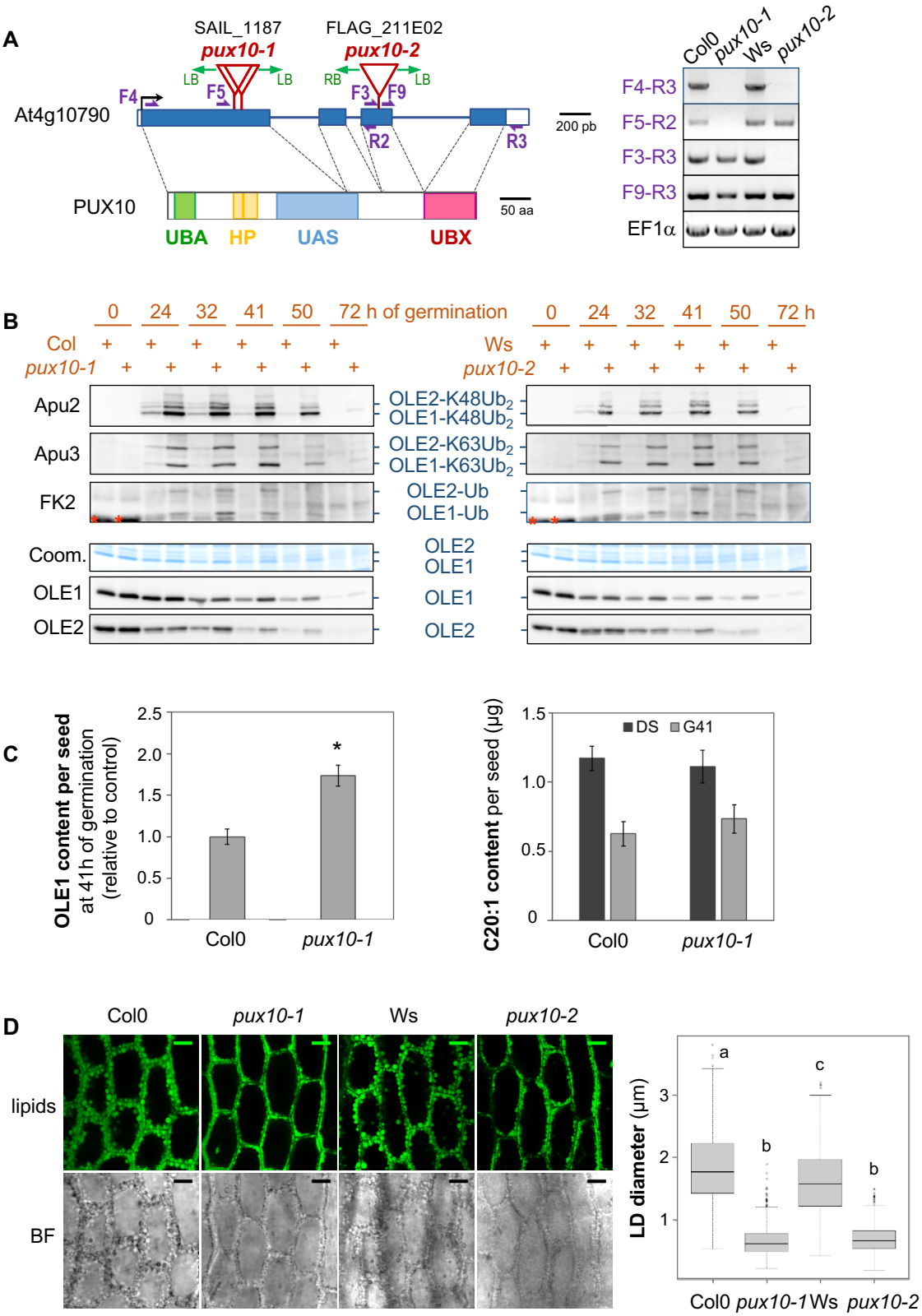
A
SAIL_1187
pux10-1
FLAG_211E02
pux10-2
LB
RB
F4
F5
F3
F9
R2
R3
At4g10790
200 pb
PUX10
50 aa
UBA
HP
UAS
UBX
Col0
pux10-1
Ws
pux10-2
F4-R3
F5-R2
F3-R3
F9-R3
EF1α
B
0
24
32
41
50
72 h of germination
Col
Ws
pux10-1
pux10-2
Apu2
Apu3
FK2
Coom.
OLE1
OLE2
OLE2-K48Ub2
OLE1-K48Ub2
OLE2-K63Ub2
OLE1-K63Ub2
OLE2-Ub
OLE1-Ub
OLE2
OLE1
C
OLE1 content per seed
at 41h of germination
(relative to control)
Col0
pux10-1
C20:1 content per seed (µg)
DS
G41
D
Col0
pux10-1
Ws
pux10-2
lipids
BF
LD diameter (µm)
a
b
c
b

Figure 1. *PUX10* mutation alters LD dynamics in germinated seeds.
(A) Molecular characterization of two *pux10* mutants. Top left panel shows a schematic representation of *PUX10* gene (At4g10790) with exons represented by blue boxes. Bottom left panel displays the domain architecture of PUX10 protein showing the UBA-like domain in green (M^{1}-S^{44}), the hydrophobic sequences of the HP domain in yellow (I^{102}-V^{117} and A^{120}-F^{141}), the UAS domain in blue (L^{170}-R^{295}) and the UBX domain in pink (E^{398}-I^{477}). The position of the *pux10-1* and *pux10-2* T-DNA insertion mutations is indicated by red triangle on the gene schematics. Sequenced T-DNA borders are indicated by green arrow (RB, right border; LB, left border). Note that the *pux10-1* T-DNA insert is flanked by two LB borders. Accumulation of *PUX10* mRNA in mutant and corresponding wild-type backgrounds was analyzed by RT-PCR on 24-h-germinated seedlings (right panel) using primers indicated as purple arrows on the *PUX10* gene structure (primer sequences are listed in Supplemental Table 1). EF1αA4 (EF1) gene expression was used as a constitutive control.
(B) *PUX10* mutation induces the accumulation of all three types of ubiquitinated oleosins and slows down the degradation of oleosins during post-germinative growth. Proteins were extracted from mutant and wild-type seeds/seedlings at various stages of germination (0 to 72 h). The three types of ubiquitin-oleosin conjugates were detected by immunoblotting with anti-ubiquitination antibodies (Apu2, specific to K48-linked polyubiquitinated proteins; Apu3, specific to K63-linked polyubiquitinated proteins; FK2, detecting monoubiquitinated proteins). Oleosin content was analyzed by SDS-PAGE followed by Coomassie blue staining (Coom.) or immunoblotting with anti-OLE1 or anti-OLE2 serum (OLE1 or OLE2). Total protein extracts from an equivalent amount of seedlings were loaded on each lane. Red asterisks mark non specific labeling of seed storage proteins in FK2 immunoblot.
(C) Oleosin degradation associated to post-germinative growth is reduced in *pux10-1* mutant. Col0 and *pux10-1* seeds were germinated in water for 41 h. OLE1 content per seedling was measured using quantitative immunoblot (mean ± SD from four independent seed batches). The asterisk indicates a significant genotype difference (Kruskal-Wallis test; $p < 0.02$). Eicosanoic acid (C20:1), a marker for storage oil, was measured by gas chromatography on the same batches of 41-h-old seedlings (G41) and compared to mature dry seed content (DS). C20:1 content was not significantly different in *pux10-1* compared to wild-type Col0 (n=16; four samples of 30 seeds / seed batch x four independent seed batches) as determined by Kruskal-Wallis test ($p > 0.05$).
(D) *PUX10* mutation prevents the increase in lipid droplet (LD) size occurring during early seedling growth. LDs of 32-h-old seedlings were stained with LipidTOX Deep Red and visualized in the hypocotyl epidermis next to the radicle by fluorescent CLSM (green) and bright-field (BF) microscopy (grey). Representative images of *pux10-1* and *pux10-2* seedlings are compared with those of Col0 and Ws seedlings. Scale bars represent 10 µm. The boxplot with Tukey-style whiskers shows the LD diameter distribution of *pux10-1*, *pux10-2* and respective wild-type seedlings. Black lines represent medians, top and bottom ends of the boxes represent the first and third quartiles, respectively. Letters above the boxes indicate groups with significant differences as determined by *t*-test ($p<0,0001$; $n>450$ from 3-4 individuals).

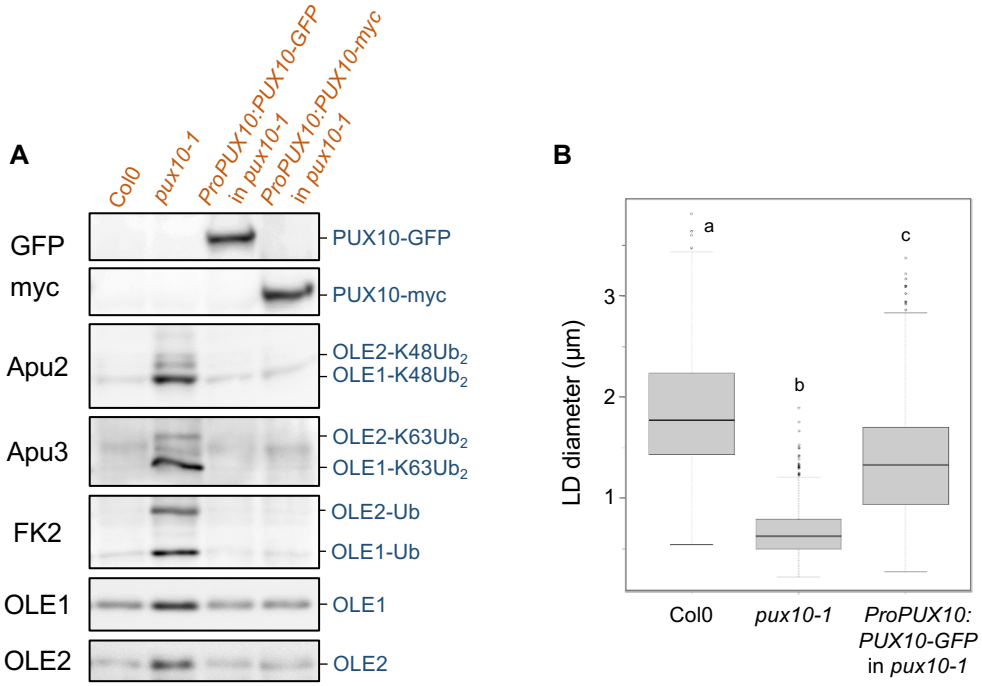

Figure 2. Stable expression of PUX10-GFP or PUX10-myc rescues the phenotype of *pux10-1*.
(A) Expression of PUX10-GFP or PUX10-myc restores the ability to degrade ubiquitinated oleosins in *pux10-1* seedlings. Seeds from Col0, *pux10-1*, and stable Arabidopsis *ProPUX10:PUX10-GFP*/*pux10-1* and *ProPUX10:PUX10-myc*/*pux10-1* transgenic lines were germinated for 41 h. Proteins were extracted from seedlings and analyzed by immunoblot with anti-GFP, anti-myc, Apu2, Apu3, FK2, anti-OLE1, and anti-OLE2 antibodies to detect PUX10-GFP, PUX10-myc, OLEs-K48Ub_2, OLEs-K63Ub_2, OLEs-Ub, OLE1, and OLE2, respectively. Total protein extracts from an equivalent amount of seedlings were loaded on each lane.
(B) PUX10-GFP expression partially restores LD morphology in *pux10-1* mutant. The boxplot shows the distribution of LD diameters measured in 32-h-old seedlings of the *ProPUX10:PUX10-GFP*/*pux10-1* transgenic line, compared to those of *pux10-1* and Col0 (reported from Figure 1D). Letters above the boxes indicate groups with significant differences as determined by *t*-test ($p<0{,}0001$; $n>450$ from 3 individuals).

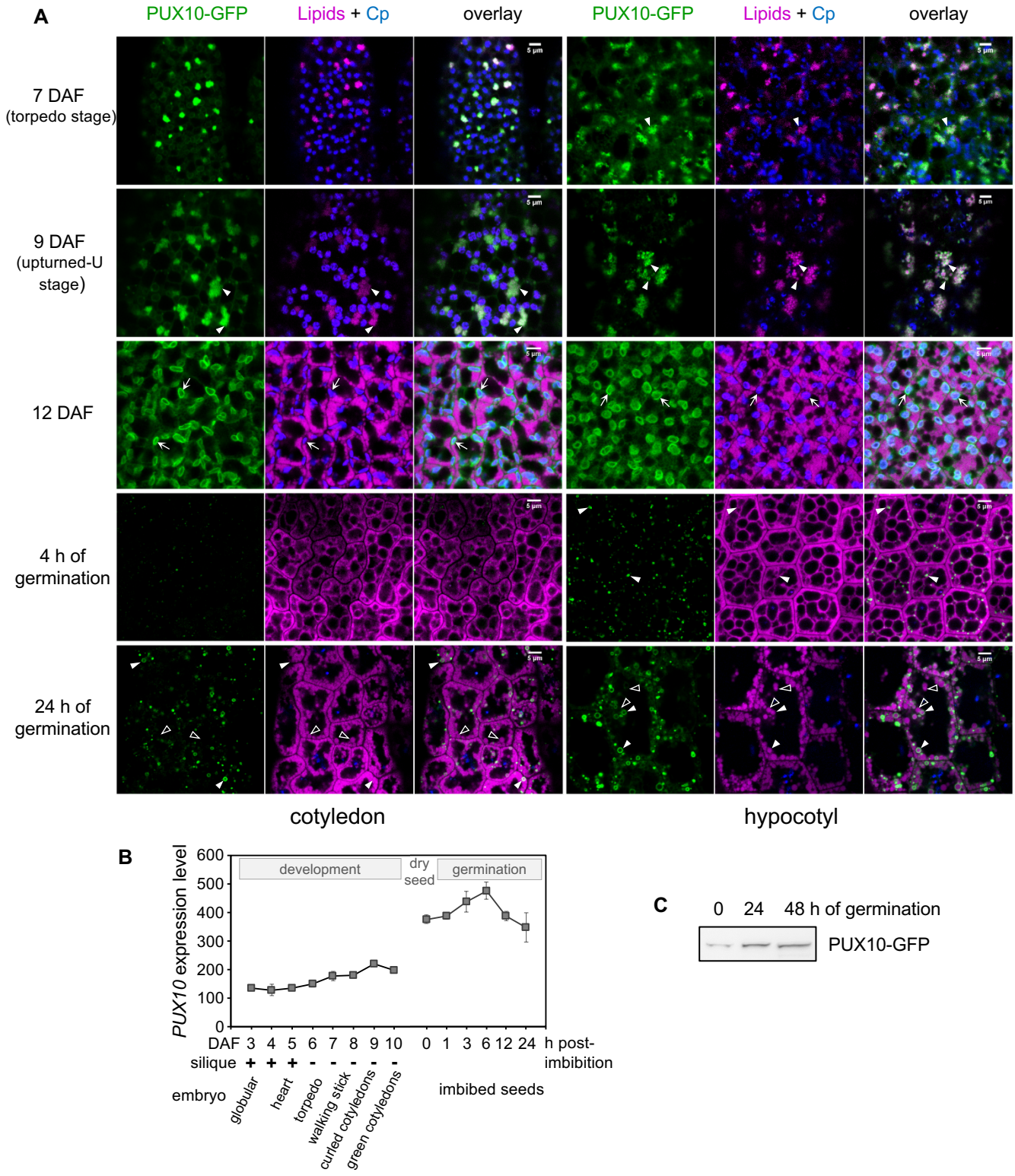

Figure 3. Changes in PUX10 expression and localization during seed development and germination.
(A) PUX10 localizes to LDs during embryo morphogenesis and seed germination, and to chloroplast membranes during seed maturation. Stable Arabidopsis *ProPUX10:PUX10-GFP*/*pux10-1* transgenic line was analyzed by confocal microscopy. Cotyledon and hypocotyl epidermises were imaged at different stages of seed development (embryogenesis at 7 and 9 days after flowering (DAF), maturation at 12 DAF) and seed germination (4 and 24 h of germination). LDs were visualized by LipidTOX Deep Red staining (magenta). Blue color shows chloroplast (Cp) autofluorescence. In embryos and germinating seeds, the ring-shaped labeling of PUX10-GFP around LDs (white arrowheads) is typical of LD-associated proteins. Note the absence of PUX10-GFP on several LDs from 24h-old seedlings (empty arrowheads), showing that PUX10 is targeted to a subset of LDs during germination. Also note the dramatic change in PUX10 targeting during seed development, with PUX10 exclusively localized to LDs during embryogenesis (7-9 DAF; white arrowheads) and to chloroplast membranes at 12 DAF (arrows). Scale bar = 5 µm.
(B) Absolute expression levels of *PUX10* in developing and germinating seeds at different stages. Data were extracted from the Arabidopsis eFP browser (http://bar.utoronto.ca/efp/cgi-bin/efpWeb). Average values are shown, and the error bars represent SD.
(C) PUX10 expression increases during germination. *ProPUX10*-driven expression of PUX10 was analyzed by immunoblot. Proteins were extracted from dry mature and 24-h- and 48-h-old seedlings of Arabidopsis *ProPUX10:PUX10-GFP*/*pux10-1* transgenic line. Total protein extracts from an equivalent amount of seedlings were immunoblotted with anti-GFP antibody.

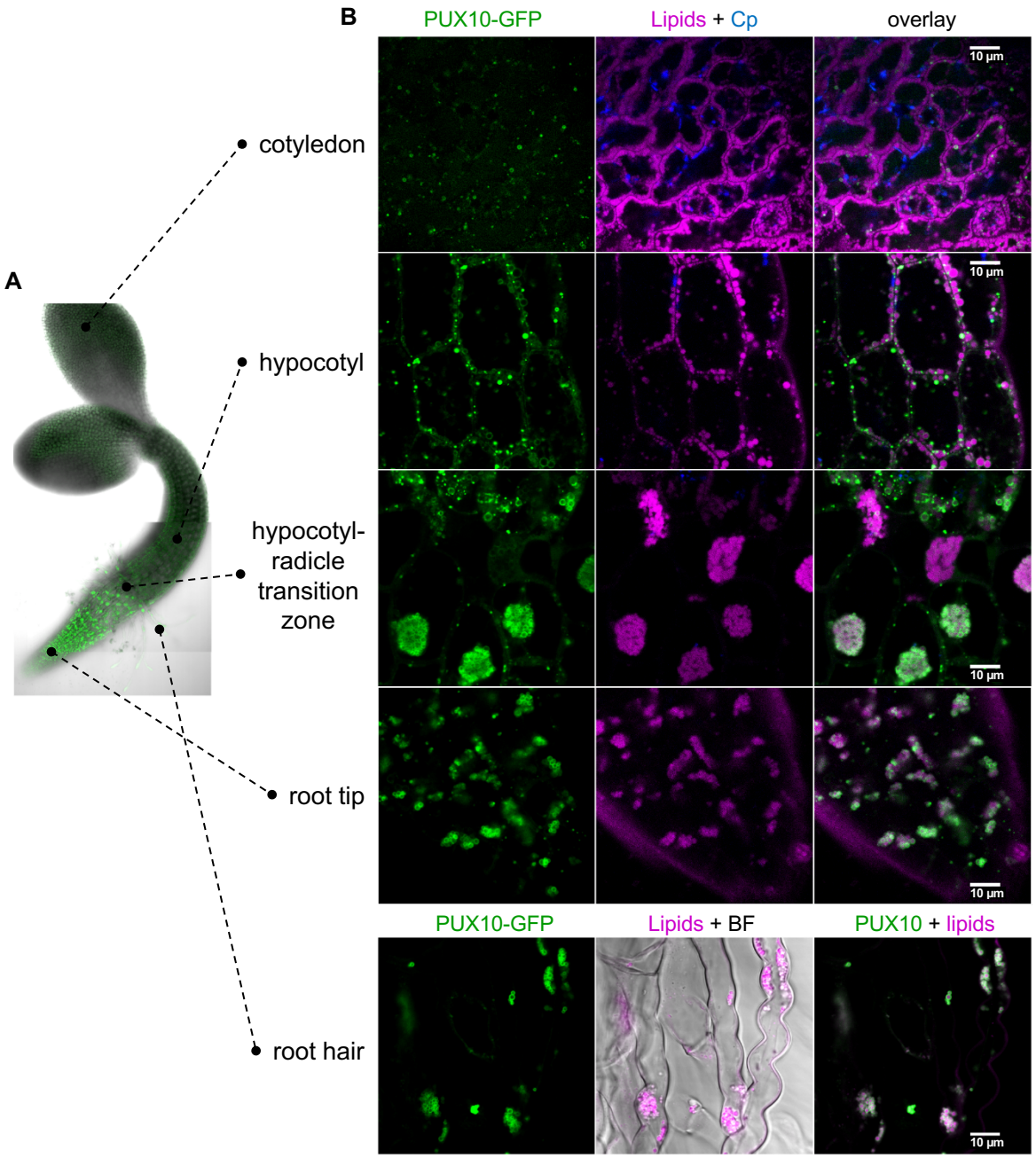

Figure 4. PUX10 localizes to LDs in the different tissues of young seedlings.
Stable Arabidopsis *ProPUX10:PUX10-GFP*/*pux10-1* transgenic seeds were germinated for 32 h, labeled with LipidTOX Deep Red to stain LDs (magenta) and imaged by confocal microscopy.
(A) Bright-field/GFP overlay image of the whole seedling was reconstituted by joining three images recorded using the same settings.
(B) Magnified images of PUX10-GFP localization in different seedling tissues. Upper central panels show chloroplast (Cp) autofluorescence (blue) merged to LipidTOX fluorescence (magenta). Lower central panel shows bright-field (BF) image merged to LipidTOX fluorescence. Scale bar = 10 µm.

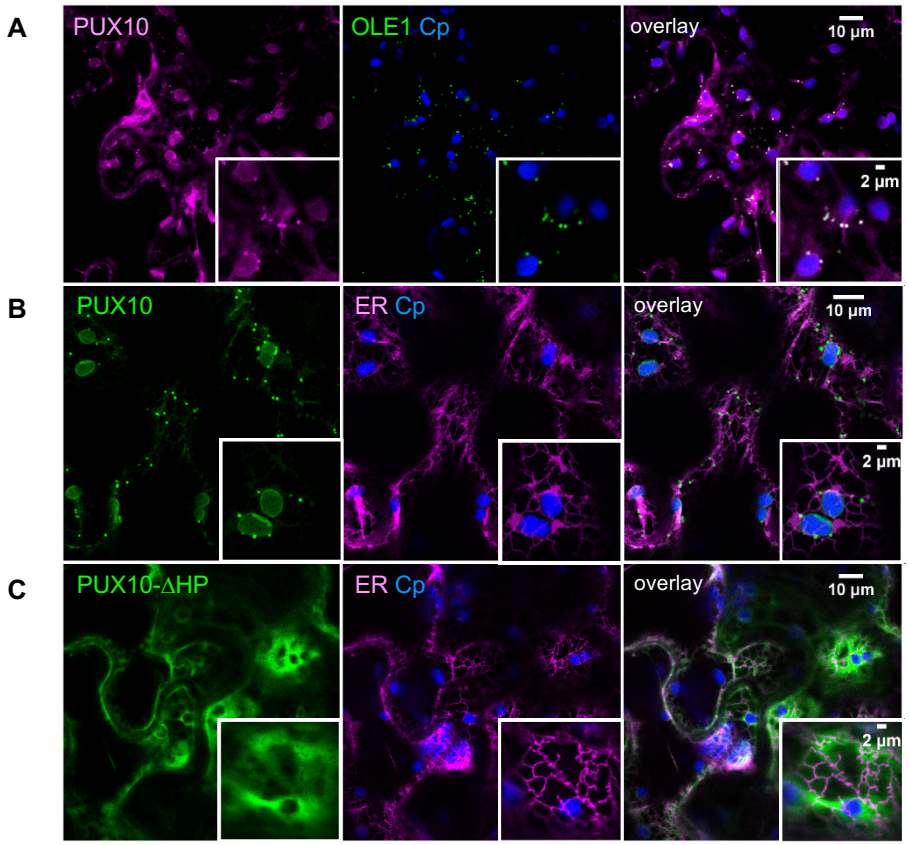

Figure 5. The HP domain of PUX10 is a membrane-anchoring domain required for PUX10 localization to LDs and chloroplast membranes.
Representative confocal images of fluorescent-tagged PUX10 transiently expressed in *N. benthamiana* leaves, with chloroplast (Cp) autofluorescence in blue. Magnified views are shown in inserts.
(A) Co-expression of mCherry-PUX10 and GFP-OLE1 (used as a LD marker) in wild-type *N. benthamiana* leaves infiltrated with pMDC32-mCherry-PUX10- and pB7WGF2-GFP-OLE1-containing agrobacteria.
(B-C) Expression of full-length (B) or HP-domain truncated (C) GFP-PUX10 in transgenic *N. benthamiana* expressing an ER resident red fluorescent protein (RFP-ER; magenta). Leaves were infiltrated with agrobacteria containing pGWB6-GFP-PUX10 (B) or pGWB6-GFP-PUX10c-ΔHP (C).

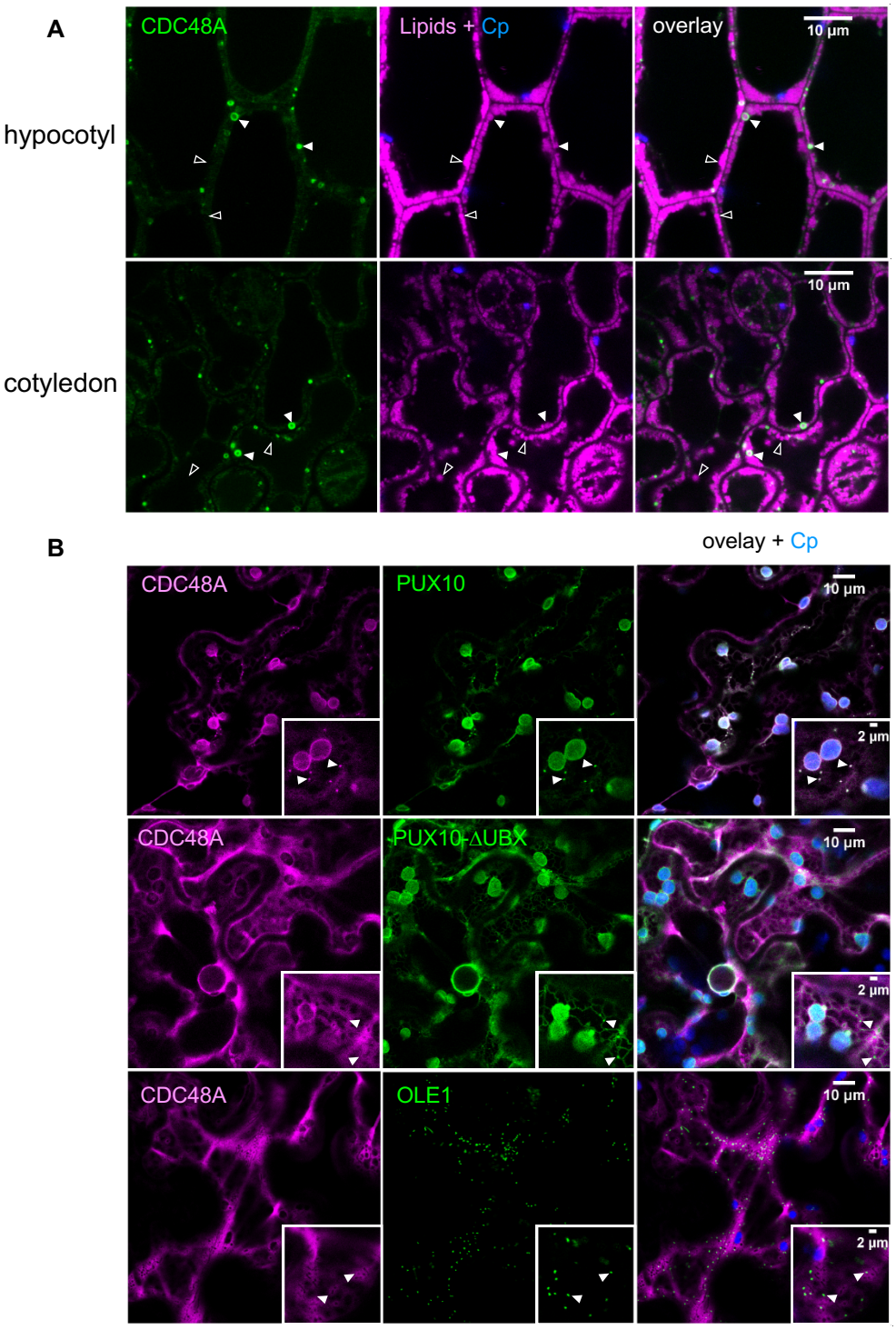

Figure 6. Localization of CDC48A to LDs.
(A) CDC48A localizes to a subset of LDs in Arabidopsis germinated seeds. Transgenic *ProCDC48A:YFP-CDC48A*/*Atcdc48A* seedlings stably expressing YFP-CDC48A (line produced by Park *et al*., 2008) were imaged by confocal microscopy (green), after LD staining with LipidTOX Deep Red (magenta). Cotyledon and hypocotyl epidermises were analyzed at 32 h of germination. Chloroplast (Cp) autofluorescence was recorded in blue and merged with LipidTOX fluorescence (upper central panels). YFP-CDC48A was associated with some but not all LDs (white and empty arrowheads, respectively).
(B) The UBX domain of PUX10 promotes CDC48A association with LDs and chloroplast membranes. Fluorescent CDC48A (mCherry-CDC48A) was co-expressed with GFP-PUX10 or GFP-PUX10-ΔUBX (lacking the UBX domain) or GFP-OLE1 (LD marker) in wild-type *N. benthamiana* leaves, after infiltration with agrobacteria containing pMDC32-mCherry-CDC48A and pGWB6-GFP-PUX10 or pGWB6-GFP-PUX10-ΔUBX or pB7WGF2-GFP-OLE1, respectively. White arrowheads show LDs in high-magnification images.

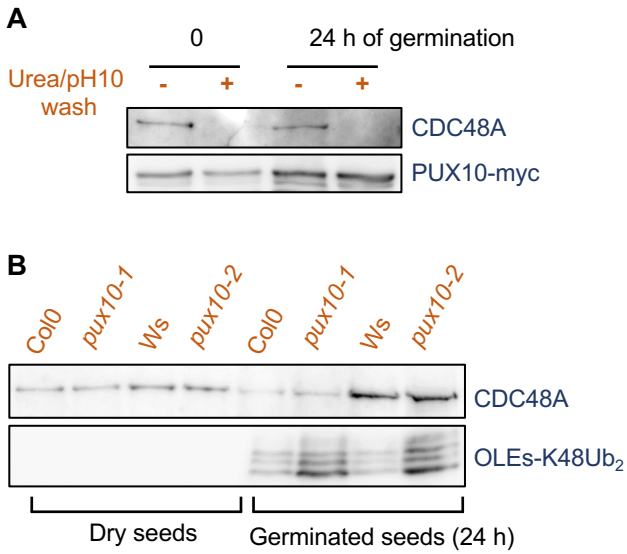

Figure 7. Characterization of CDC48A association with LDs.
(A) CDC48A is peripherally associated with LDs, whereas PUX10 is an integral protein of the LD semi-membrane. Purified LDs isolated from *ProPUX10:PUX10-myc*/*pux10-1* transgenic dry or germinated seeds were incubated in carbonate buffer (pH10) containing 8 M urea or in non-denaturing SH buffer (control). Washed LDs were re-isolated and analyzed by immunoblotting using anti-CDC48A serum or anti-myc antibody to detect CDC48A or PUX10-myc, respectively. Equivalent amounts of proteins were loaded in each lane.
(B) CDC48A association with LDs is not impaired in *pux10* mutants. LDs were isolated from *pux10-1*, Col0, *pux10-2*, and Ws dry and germinated seeds. CDC48A and OLEs-K48Ub2 were immunodetected using anti-CDC48A and Apu2 antibodies, respectively. Equivalent amounts of LD proteins were loaded in each lane.

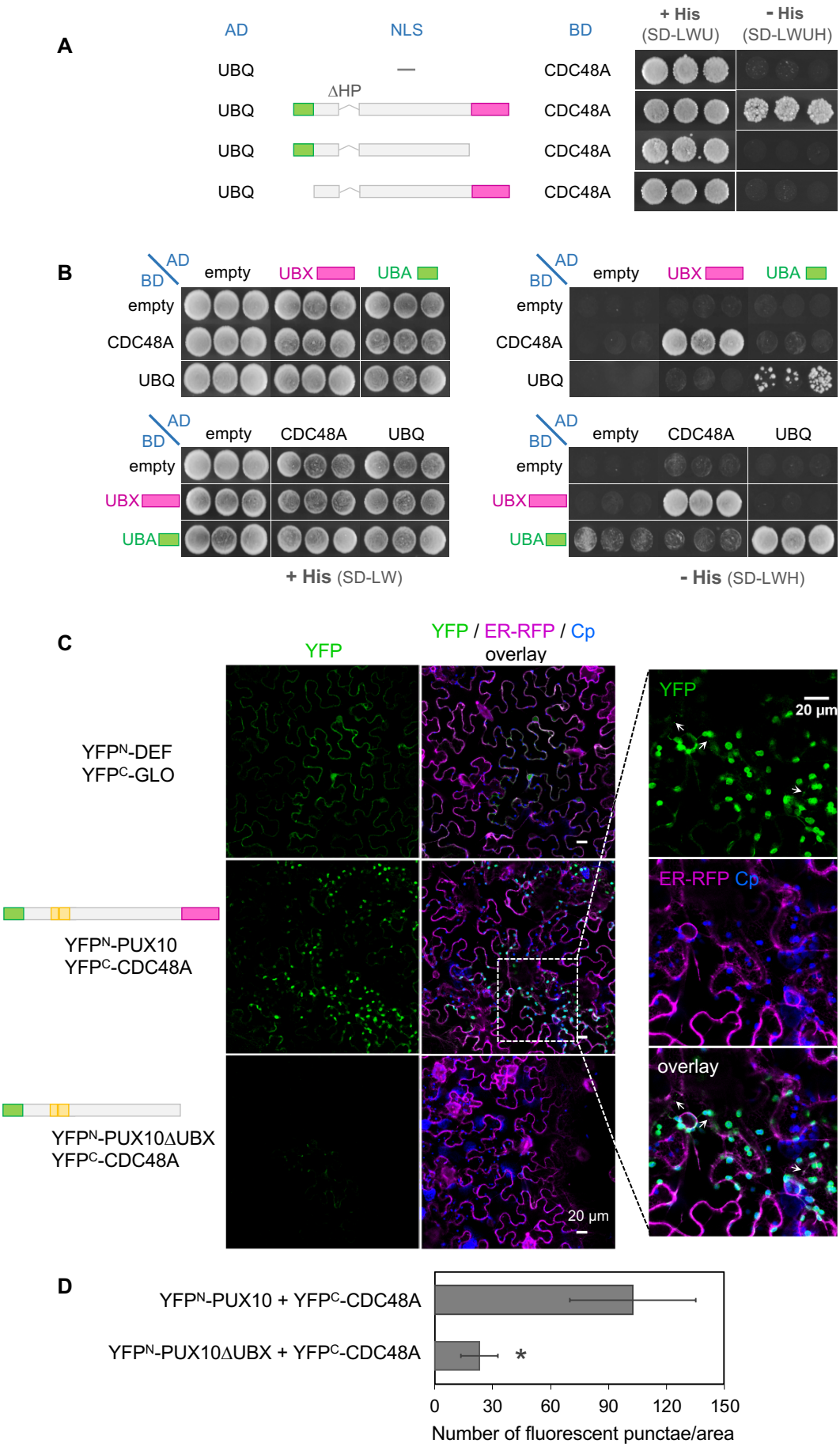
A
AD
NLS
BD
+ His (SD-LWU)
- His (SD-LWUH)
UBQ
—
CDC48A
ΔHP
B
AD
BD
empty
UBX
UBA
CDC48A
UBQ
+ His (SD-LW)
- His (SD-LWH)
C
YFP
YFP / ER-RFP / Cp overlay
YFPN-DEF
YFPC-GLO
YFPN-PUX10
YFPC-CDC48A
YFPN-PUX10ΔUBX
YFPC-CDC48A
ER-RFP Cp
overlay
20 μm
D
YFPN-PUX10 + YFPC-CDC48A
YFPN-PUX10ΔUBX + YFPC-CDC48A
*
0
30
60
90
120
150
Number of fluorescent punctae/area

Figure 8. PUX10 interacts with ubiquitin and CDC48A through its UBA and UBX domains, respectively.
(A) Ternary complex formation between ubiquitin (UBQ), PUX10 and CDC48A as determined by yeast three-hybrid assay. PUX10 lacking either the UBA or UBX domain or not, was fused to a nuclear localization signal (NLS) and co-expressed with UBQ fused to GAL4-activation domain (AD) and with CDC48A fused to GAL4-DNA binding domain (BD). The transmembrane HP domain (I^{102}-F^{141}) was deleted from PUX10 to ensure proper nuclear targeting. Interactions between three proteins were tested using the *HIS3* reporter gene by monitoring yeast growth on selective medium without histidine (-His).
(B) Mapping of the PUX10 domains interacting with UBQ and CDC48A by yeast two-hybrid assay. UBQ, CDC48A, and the UBX and UBA domains of PUX10 were used as either bait (BD fusion) or prey (AD fusion). Yeasts harboring both bait and prey expression vectors were grown on medium without His to check for interaction between both partners.
(C) *In planta* interaction between PUX10 and CDC48A visualized by bimolecular fluorescent complementation (BiFC). *Nicotiana benthamiana* epidermal cells constitutively expressing an ER resident fluorescent protein (ER-RFP, magenta) were co-infiltrated with *Agrobacterium* cultures expressing YFP-N terminus fused to PUX10 full-length (YFP^N-PUX10) or lacking the UBX domain (YFP^N-PUX10ΔUBX) and YFP-C terminus fused to CDC48A (YFP^C-CDC48A). An YFP fluorescence signal (left panel in each pair, green) reveals an interaction between the two tested fusion proteins. The right panel of each pair shows the merged signals of YFP, chloroplast autofluorescence (Cp, blue) and ER-RFP (magenta). The interaction between PUX10 and CDC48A localizes mainly to chloroplasts, but also to LDs (indicated by arrows in the magnified views). The interaction between MADS box transcription factors Deficiens (DEF) and Globosa (GLO) is shown as positive control. All confocal images have been recorded using the same settings. Scale bars represent 20 µm.
(D) Quantification of BiFC assays with PUX10 and CDC48A in *N. benthamiana* leaf cells. The graph shows the mean number (± SD) of fluorescent punctae in 6 areas of transformed epidermal cells, similar to those shown in (C). The asterisk indicates a significant difference between leaves infiltrated with *Agrobacterium* cultures expressing YFP^C-CDC48A and YFP^N-PUX10, or YFP^C-CDC48A and YFP^N-PUX10ΔUBX ($p<0,002$; as determined by *t*-test).

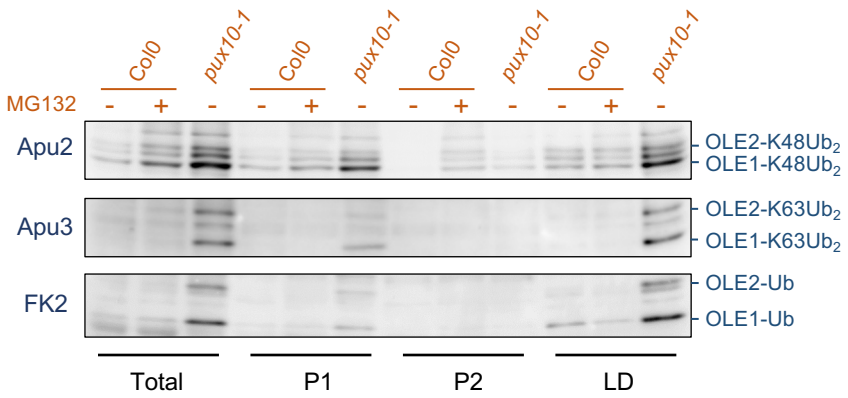

Figure 9. The dislocation of ubiquitinated oleosins from LDs is prevented in *pux10-1* mutant. Arabidopsis *pux10-1* or Col0 seeds were germinated for 41 h in water containing 0.2% DMSO as a solvent control or 100 µM MG132. Seedling homogenates (Total) were centrifuged at 1,000 x *g* to remove cell debris (pellet P1) and then fractionated by centrifugation into three fractions (25,000 x *g* pellet, P2; floating fat layer containing LDs, LD; the soluble fraction was not analyzed because oleosins are water insoluble). Protein samples fractionated from an equivalent number of seedlings were loaded on each lane and analyzed by immunoblotting with the anti-ubiquitination antibodies Apu2, Apu3, or FK2.

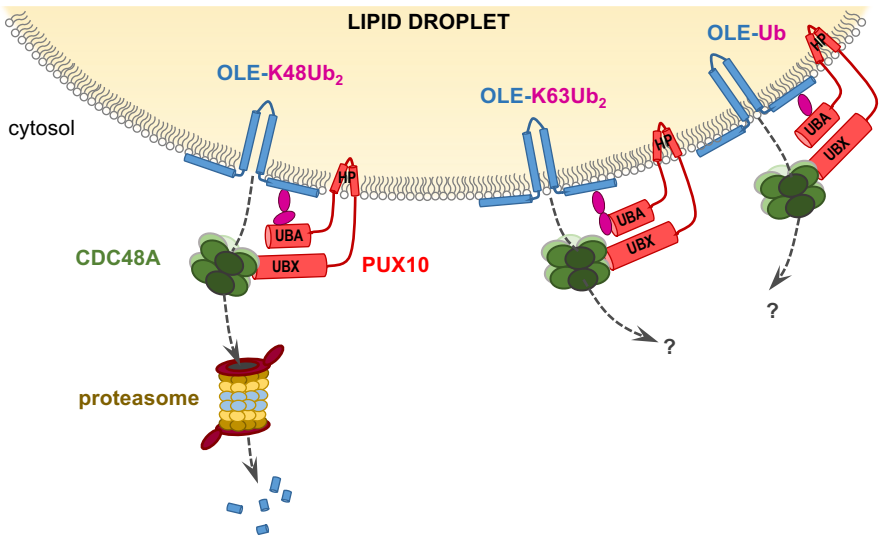

Figure 10. A model of the LD-associated degradation (LDAD) pathway.
Oleosins (OLEs) are marked for degradation by the addition of either a monoubiquitin (Ub), a K48-linked diubiquitin ($K48Ub_2$) or a K63-linked diubiquitin ($K63Ub_2$). The E2 ubiquitin-conjugating and E3 ligase enzymes involved in oleosin ubiquitinations are yet unknown. In germinating seeds, PUX10 associates with LDs through its hydrophobic HP domain. PUX10 bridges the CDC48A segregase to ubiquitinated oleosins through its UBX and UBA domains, respectively, to promote the dislocation of all three types of ubiquitinated oleosins from the LD semi-membrane. Once dislocated from the LD surface, $K48Ub_2$-conjugated oleosins are degraded by the proteasome. The fate of Ub- and $K63Ub_2$-conjugated oleosins is currently undetermined.